HHS Public Access

Author manuscript

Cell. Author manuscript; available in PMC 2024 October 26.

Published in final edited form as:

Cell. 2023 October 26; 186(22): 4788–4802.e15. doi:10.1016/j.cell.2023.09.014.

Amyloplast sedimentation repolarizes LAZYs to achieve gravity sensing in plants

Jiayue Chen[1,2,3,7,8], **Renbo Yu**[2,4,7], **Na Li**[1,3,7], **Zhaoguo Deng**[1,3,7], **Xinxin Zhang**[2,7,9], **Yaran Zhao**[1,2,3,7,8], **Chengfu Qu**[1,3,7], **Yanfang Yuan**[2], **Zhexian Pan**[1,3], **Yangyang Zhou**[2], **Kunlun Li**[2], **Jiajun Wang**[2], **Zhiren Chen**[1,3], **Xiaoyi Wang**[2], **Xiaolian Wang**[1,3], **Shu-Nan He**[1,3], **Juan Dong**[5,6], **Xing Wang Deng**[2], **Haodong Chen**[1,2,3,10,*]

[1]Center for Plant Biology, School of Life Sciences, Tsinghua University, Beijing 100084, China

[2]State Key Laboratory of Protein and Plant Gene Research, School of Advanced Agricultural Sciences and School of Life Sciences, Peking-Tsinghua Center for Life Sciences, Peking University, Beijing 100871, China

[3]Tsinghua-Peking Center for Life Sciences, Beijing 100084, China

[4]Key Laboratory of Vegetable Research Center, Tropical Crops Genetic Resources Institute, Chinese Academy of Tropical Agricultural Sciences, Haikou 571101, China

[5]The Waksman Institute of Microbiology, Rutgers, the State University of New Jersey, Piscataway, New Jersey, 08854, USA

[6]Department of Plant Biology, Rutgers, the State University of New Jersey, New Brunswick, New Jersey, 08901, USA

[7]These authors contributed equally

[8]Present address: Veminsyn Biotechnology Ltd., Hangzhou 310000, China

[9]Present address: State Key Laboratory of Systematic and Evolutionary Botany, Institute of Botany, Chinese Academy of Sciences, Beijing 100093, China

[*]Correspondence: chenhaodong@tsinghua.edu.cn.

AUTHOR CONTRIBUTIONS

H.C. conceived and supervised the study. Y.Y., R.Y., and K.L. generated and analyzed *lazy* triple mutants in Col. and *DR5rev::GFP*. R.Y., Y. Zhao, X.Z., J.C., J.W., and X.Y.W. generated the LAZY-GFP lines and collected the fluorescence data. N.L. carried out the immuno-electron microscopy. J.C. carried out the protein-lipid overlay assay. Y.Zhao, X.Z., X.L.W., and Z.D. generated and analyzed truncated LAZY-GFP lines. Y. Zhao, N.L., and Z.P. generated and analyzed LAZY-GFP/*pgm1* lines. Z.D. carried out the 3-D reconstruction and FRAP experiments. J.C. and C.Q. carried out IP-MS, and performed the *in vitro* phosphorylation and interaction assay. S.-N.H., J.C., N.L., Z.C. and Z.D. generated and analyzed the LAZY4-GFP*/mpk* line. Z.D., J.C., Y. Zhou, N.L., Z.C. and Z.P. generated and analyzed LAZY4-A13-GFP and LAZY4-D9-GFP lines. Y. Zhao, N.L., R.Y., J.C., and Z.P. performed the yeast two hybrid analysis. N.L. generated and analyzed LAZY4-GFP/*toc* and LAZY4-D9-GFP/*toc* lines with the help of X.L.W. Z.D. did multiple analyses about fluorescence, phenotypes, and MS data. H.C., Z.D., J.C., R.Y., N.L., Y.Zhao, J.D. and X.W.D. drafted the manuscript.

DECLARATION OF INTERESTS

The authors declare no competing interests.

SUPPLEMENTAL INFORMATION

Supplemental information can be found online.

[10]Lead contact

SUMMARY

Gravity controls directional growth of plants, and the classical starch-statolith hypothesis proposed more than a century ago postulates that amyloplast sedimentation in specialized cells initiates gravity sensing, but the molecular mechanism remains uncharacterized. The LAZY proteins are known as key regulators of gravitropism and *lazy* mutants show striking gravitropic defects. Here, we report that gravistimulation by reorientation triggers Mitogen-Activated Protein Kinase (MAPK) signaling-mediated phosphorylation of *Arabidopsis* LAZY proteins basally polarized in root columella cells. Phosphorylation of LAZY increases its interaction with several Translocons at the Outer envelope membrane of Chloroplasts (TOC) proteins on the surface of amyloplasts, facilitating enrichment of LAZY proteins on amyloplasts. Amyloplast sedimentation subsequently guides LAZY to relocate to the new lower side of the plasma membrane in columella cells, where LAZY induces asymmetrical auxin distribution and root differential growth. Together, this study provides a molecular interpretation for the starch-statolith hypothesis: the organelle movement-triggered molecular polarity formation.

In brief

Amyloplast sedimentation guides LAZY to relocate to the new lower side of the plasma membrane in columella cells to induce gravitropic growth in plants.

Graphical Abstract:

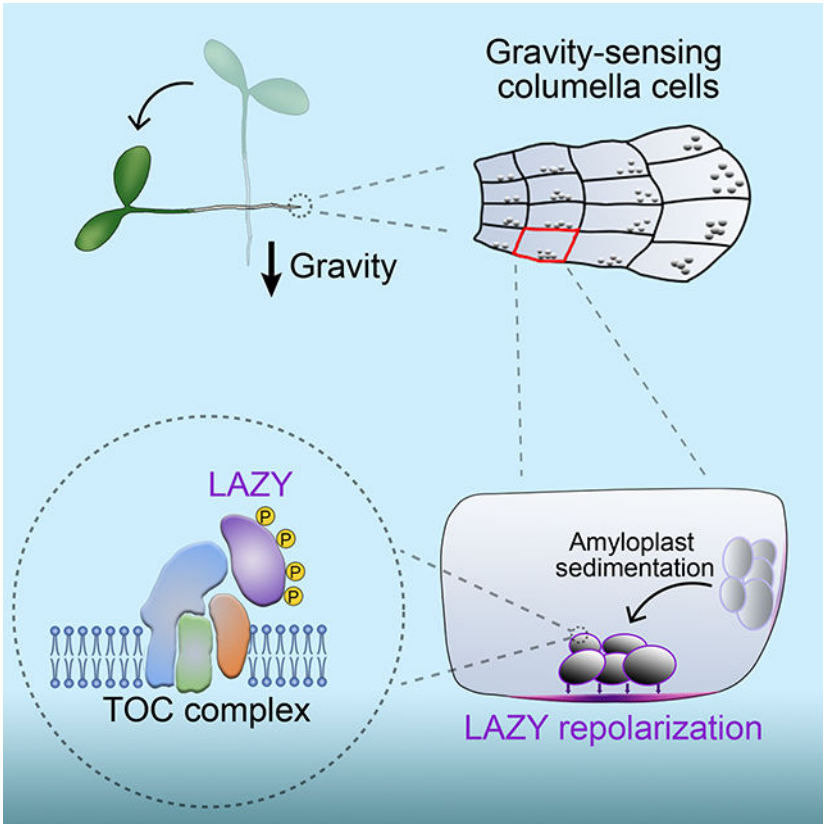

Keywords

Gravitropism; Starch-statolith hypothesis; Amyloplast sedimentation; polarity; Phosphorylation; LAZY; TOC; MPK

INTRODUCTION

Gravity is a key environmental factor acting on all organisms on earth. In plants, gravity usually directs roots to grow downwards (positive gravitropism) and aerial parts to grow upwards (negative gravitropism) [1,2], which may control agricultural traits such as drought tolerance[3], nutrient absorption[4], and so on. Gravitropism includes three key processes: gravity sensing, signal transduction, and differential growth response[2,5]. Since the direction and the magnitude of gravity are almost constant on the surface of the earth, gravitropism is regarded as a posture control, triggered by sensing the tilt of organs relative to the direction of gravity vector[5].

The starch-statolith hypothesis and Cholodny-Went theory are the dogmas for explaining gravity sensing and response, respectively[6]. The starch-statolith hypothesis was proposed one hundred and twenty years ago, in which sedimentation of amyloplasts (starch-filled plastids) in the statocytes was considered to initiate gravity sensing[7–9]. The columella cells in roots and endodermal cells in shoots were demonstrated to be the statocytes for sensing gravity, and genetic disruption or laser ablation of these cells led to complete disruption of

the gravitropism[10–12]. Gravity sensing is further divided into susception (physical response) and signal conversion from physical to physiological information[5]. The sedimentation of starchless plastids in *phosphoglucomutase 1* (*pgm1*) mutants was impaired, resulting in a slower gravitropic response in both roots and shoots[13,14]. In contrast, disruption of actin accelerated amyloplast sedimentation, resulting in promoted gravitropism[15]. Generally, amyloplast sedimentation was considered to be the susception step of gravity sensing[5], but the molecular roles of amyloplast sedimentation and the underlying mechanisms of signal conversion were unclear. The Cholodny-Went theory proposed that growth curvature is due to an unequal distribution of auxin between the two sides of the curving organ in plants[16], and auxin efflux transporter PIN proteins were later proved to contribute to the redirection of auxin and subsequent differential growth in gravitropism[17,18].

In the 1930s, an unusual corn mutant with a stalk growing towards the ground was described as "*lazy*" due to its prostrate phenotype (sleeping stature) [19,20]. The rice *lazy* mutant with a similar phenotype was identified later[21]. Since then, the *LAZY* family genes were demonstrated to be critically important for the gravitropic responses of both shoots and roots in many plant species, including, rice[3,21–23], maize[20,24], *Arabidopsis*[25–27], *Medicago truncatula*[28], *Prunus domestica*[26] and *Lotus japonicus*[29]. High-order *lazy* mutants in *Arabidopsis* showed more exaggerated phenotypes than single mutants, though the phenotypes reported by different groups varied[28,30,31]. Our previous study showed that light modulates gravitropism by controlling the expression level of *LAZY4*[32]. A recent study showed that *Arabidopsis* LAZY4 (LZY3) proteins display polar distribution on the plasma membrane of the columella cells in lateral roots, and recruit RCC1-like domain (RLD) proteins from the cytoplasm to the plasma membrane to promote the re-localization of PIN3 and modulate auxin flow[33]. LAZY4 (AtDRO1) has also been reported to show nuclear localization, but its role there is unclear[34].

Altered Response to Gravity 1 (*ARG1*) encodes a DnaJ-like protein and its mutation delayed gravitropism in both root and hypocotyl[35]. Mutating *TOC34*, *TOC75*, *TOC120* or *TOC132*, components of the Translocons at the Outer envelope membrane of Chloroplasts (TOC) complexes, significantly enhanced the *arg1* gravitropic defect, even though either *toc132*^{Q730Stop}, *toc75*^{G658R}, or *arg1* single mutants showed weak to no gravitropic phenotypes[36,37]. The classical function of TOC proteins is to import proteins into the plastids[38–41], but whether TOC proteins regulate gravitropism by importing unknown signal factors into amyloplasts is unclear[37].

Mitogen-Activated Protein Kinase (MAPK) cascades are highly conserved in eukaryotic cells. In plants, the MAPK signaling modules regulate many aspects of growth and environmental responses[42]. The MKK4/MKK5-MPK3/MPK6 module regulates stomatal development and patterning[43], the inflorescence architecture[44], lateral root development[45], and so on. The MKK7-MPK6 module positively regulates hypocotyl gravitropism[46].

Here, we report that gravistimulation triggers the MKK5-MPK3 module to phosphorylate LAZY proteins, which may promote LAZY proteins to enrich on the surface of amyloplasts via interacting with the TOC proteins. Then, amyloplast sedimentation promotes the translocation of LAZY proteins to the new lower side of the plasma membrane in columella

cells, in which relocation of LAZY proteins from the surface of amyloplasts to the adjacent plasma membrane is an important process. The repolarization of LAZY proteins leads to asymmetric auxin distribution and ultimately differential growth. Thus, our study reveals the molecular role of amyloplast sedimentation, providing insights into the molecular mechanism of the starch-statolith hypothesis.

RESULTS

LAZY2, 3, and *4* are requisite for the gravitropic responses in roots

Previous studies showed that simultaneously disrupting *LAZY2* (*NGR1*), *LAZY3* (*NGR3*) and *LAZY4* (*NGR2*) in *Arabidopsis* via combined T-DNA insertions in the Col or Ws ecotypes resulted in various root gravitropism phenotypes, from negative gravitropism to no clear gravitropism, probably due to the complex ecotype backgrounds or growth conditions[28,31]. To further understand the functions of LAZY family members, we used a CRISPR/Cas9 system to generate *Arabidopsis lazy2 lazy3 lazy4* (*lazy234*) triple mutants in the Col background. Three lines with different mutated alleles in the three *LAZY* genes were established for phenotypic analyses, designated *lazy234-1*, *lazy234-2* and *lazy234-3* (Figure S1A). With regards to gravitropism growth, either under white light or in the dark, primary roots of wild-type plants always grew towards the gravity vector, whereas those of *lazy234* mutants grew randomly in all directions (Figures 1A and 1B), so did the lateral roots in *lazy234* (Figures S1B and S1C). Our results are generally consistent with a previous study showing that the roots of the *atlazy2,3,4* triple mutants generated by crossing T-DNA insertion lines were agravitropic under white light and displayed weakly negative gravitropism in the dark[31]. Although the genetic distinction and possible variation of growth conditions resulted in slight phenotypic differences, our and previous data all support that these three LAZYs are essential for positive gravitropism of roots. With regards to the amyloplast sedimentation after reorientation, similar behaviors were observed in wild-type and *lazy234* mutants (Figures S1D and S1E), indicating that these LAZYs are dispensable for amyloplast sedimentation. As the asymmetric distribution of auxin promotes root gravitropism[47], and *DR5rev::GFP* is widely used to indicate auxin distribution[48], we mutated *LAZY2, LAZY3,* and *LAZY4* in the *DR5rev::GFP* reporter line via CRISPR, resulting in losing gravitropic responses in roots (Figures S2A–S2D). After the gravistimulation via reorientation, *DR5rev::GFP* signals completely lost their differential distribution in *DR5rev::GFP/lazy234* plants compared with wild-type (Figures 1C, 1D, S2E and S2F). Thus, these LAZY proteins are essential for gravity-triggered polar auxin distribution and bending responses in both primary and lateral roots.

LAZY2, 3 and 4 proteins are localized on the amyloplasts and plasma membrane in columella cells

To study protein subcellular localization, we generated endogenous promoter-driven LAZY-GFP transgenic lines in the *lazy234* mutant background. Each of the transgenes similarly and efficiently rescued the gravitropic phenotypes of *lazy234* primary roots (Figures 1A and 1B). In roots, the three LAZY proteins were predominantly expressed in columella cells, and LAZY4 was also expressed in the endodermis (Figures 2A–2C, and S3A), consistent with the previous results of promoter-driving GUS expression[31]. More strikingly, these

LAZY proteins were not only localized on the cell periphery but also on the surface of the amyloplasts in the columella cells (Figures 2D–2F). Anti-GFP immunogold labelling confirmed the localization of LAZY proteins on the plasma membrane (Figure 2G). Since starch-statolith hypothesis proposed that amyloplast sedimentation initiates gravity sensing, the localization of LAZY proteins on the surface of amyloplasts suggested that they may play critical roles in an early stage of gravity sensing and signal transduction.

LAZY2, 3 and 4 proteins were localized on the membranes, but they have no transmembrane domain or lipid acylation modification sites that may contribute to membrane association. Previous studies proved that basic and hydrophobic (BH) regions within proteins may promote their association with membranes[49,50]. BH score analysis showed that each LAZY has potential membrane binding regions (Figure S3B). Protein-lipid overlay assays showed that these LAZY proteins could bind multiple membrane phospholipids, especially phosphatidylinositolphosphates (PIPs) (Figure 2H). Mutating amino acids K/R to A within the BH peaks of LAZY4 reduced the predicted BH score (Figures S3B and S3C), and disrupted its binding to the membrane phospholipids (Figure 2H). These results suggest that these LAZY proteins may associate with membrane via binding phospholipids.

By truncation analysis, we found that deletion of the N-terminal region (containing domain I) disrupted the amyloplast localization of LAZY2, LAZY3 and LAZY4 (Figures 2I–2K). Meanwhile, the deletion of the N-terminal region disrupted the functions of these LAZYs in complementing the gravitropic defects of *lazy234* mutants (Figures 2L–2N). These data indicate that proper localization of LAZY proteins on the amyloplasts may be critical for their function in gravitropism.

Sedimentation of amyloplasts promotes the gravity-triggered redistribution of LAZY proteins

Since LAZY proteins were preferentially localized on the lower side of the plasma membrane in columella cells (Figures 2D–2F), we studied the redistribution of LAZY proteins under the regulation of gravity in both primary and lateral roots. Results showed that gravistimulation by re-orientating plants 90° could trigger re-polarization of all three LAZY proteins in columella cells of primary roots, with more proteins accumulated on the new lower side than the upper side (Figures 3A–3D, S3D and S3E). Consistently, in the columella cells of lateral roots, these LAZY proteins also displayed polarization and repolarization after re-orientating the seedlings 180° (Figures S3F and S3G).

We further studied whether the repolarization site of LAZY is related to where the amyloplasts sediment in the columella cells. Because LAZY3-GFP showed a strong amyloplast-localized fluorescence signal in our obtained transgenic lines, it was selected as the representative for detailed analysis. After the seedlings were rotated 90° or 180°, we found that redistributed LAZY3-GFP proteins to the new lower side of the columella cells highly correlated with where the amyloplasts sediment (Figures 3E–3H). Similar correlation was also observed for LAZY2-GFP and LAZY4-GFP (Figure S4A). Furthermore, to corroborate this correlation, we analyzed the distribution of LAZY proteins in the *pgm1* mutant. Indeed, mutation of *PGM1* clearly delayed the sedimentation of plastids after 90° or 180° rotation and we observed slower redistribution of LAZY proteins to the new lower

side of the columella cells (Figures 3I–3L). Further statistical analysis clearly showed that gravistimulation-induced polar redistribution of LAZY2, 3, and 4 were all delayed in the *pgm1* mutant (Figures 3M–3O, and S4B). These results suggest that the sedimentation of amyloplasts promote the redistribution of LAZY proteins after gravistimulation.

LAZY proteins translocate from the amyloplasts to the plasma membrane

In 2-D observation, multiple data showed that LAZY proteins were preferentially localized on the plasma membrane regions adjacent to amyloplasts (Figures 2D–2F, 3A–3C, 3E, 3G). To further confirm this conclusion, we rotated LAZY3-GFP seedlings 90° for gravistimulation, and collected the Z-series images when the amyloplasts were close to the new lower side of the columella cells. 3-D reconstruction of the fluorescence in columella cells showed that LAZY3-GFP proteins were only localized on the plasma membrane close to where amyloplasts were present (Figure 4A, Video S1). Further, we photo-bleached the fluorescence of LAZY3-GFP on the plasma membrane in columella cells, and found that the fluorescence in the lower side of the plasma membrane could be recovered rapidly in the columella cells with unbleached amyloplast fluorescence (LOI1, Figures 4B–4D, Video S2). In contrast, fluorescence recovery at the same position was much slower in the columella cells with bleached amyloplast fluorescence (LOI2, Figures 4B–4D, Video S2). These data indicate that LAZY proteins can be translocated from amyloplasts to the adjacent plasma membrane.

Gravistimulation induces phosphorylation of LAZY4 via MKK5-MPK3

To study how gravistimulation mediates the translocation of LAZY proteins, we performed Immunoprecipitation-Mass Spectrometry (IP-MS) analysis using LAZY4-GFP as the representative due to its highest expression level (based on fluorescence) among the three LAZYs. LAZY4-GFP seedlings were grown vertically or treated with gravistimulation (5 min, 10 min, 0.5 h, 2 h and 24 h) for phospho-proteomic analysis. The mass spectrometric analysis identified 10 phosphorylation sites in total, most of which showed up-regulated phosphorylation levels after gravistimulation (Figure S5 and Table S1). Phosphorylated peptide “FLNCPSSLEVDR” containing phosphorylation sites S139/S140 could be detected stably in all the replicates, thus it was selected as the representative to show the details of mass spectrometry results. Phosphorylation levels of this peptide were clearly induced by gravistimulation but returned to the original status after 24 h (Figure 5A and Table S2). Furthermore, to identify possible kinases, we searched the IP-MS data of LAZY4-GFP and found the protein abundance of two kinases, MPK3 and MKK5, was increased dramatically after gravistimulation and decreased to the original level after 24h (Figure 5B and Table S3), a pattern highly similar to the phosphorylation dynamics of LAZY4 (Figure 5A). Since 5-min gravistimulation was already sufficient to induce a strikingly increased association of MPK3 to LAZY4, as well as increased phosphorylation level of LAZY4 (Figures 5A and 5B), the phosphorylation of LAZY4 may take place shortly (within 5 min) after gravistimulation. Additionally, the MPK3 proteins co-immunoprecipitated by LAZY4 are highly phosphorylated (Figure 5C and Table S4). Consistently, *in vitro* pull-down experiments also showed that the interactions of LAZY4 with MPK3 and MKK5 were detectable only after the incubation with both kinases (Figure 5D). *In vitro* phosphorylation assay confirmed that MKK5-activated MPK3 can phosphorylate LAZY4,

and the phosphorylation sites matched well with the phosphorylation sites in plants (Figure 5E and Table S1). These data suggest that gravistimulation rapidly induces the phosphorylation of LAZY4 by MKK5 and MPK3.

MPK3 and MPK6 are often functionally redundant in regulating developmental processes and the null allele of the double mutant is seedling lethal[43]. To evaluate the regulation of LAZY4 by MPK3 and MPK6 in plants, we reduced the expression of *MPK3* via inducible RNAi in *mpk6* using the *mpk6*$^{-/-}$*mpk3RNAi*-est line[45]. We found that the double mutants disrupted the localization of LAZY4-GFP onto the surface of amyloplasts and polar redistribution of LAZY4-GFP on the plasma membrane under gravistimulation (Figures 5F and 5G), resulting in delayed gravitropic response (Figure 5H). Further, we mutated all 13 phosphorylation sites identified in plants and by *in vitro* kinase assays to be Ala (A) (Figure S5 and Table S1), which was named as LAZY4-A13, a phosphodead version of LAZY4. We transformed LAZY4-A13-GFP into the *lazy234* mutant, and selected the lines with fluorescence intensity comparable to LAZY4-GFP for further analysis. Like the effects of the mutation of *MPK3* and *MPK6*, these mutations on phosphorylation sites disrupted the localization of LAZY4-A13-GFP onto the surface of amyloplasts and polar redistribution of LAZY4-A13-GFP on the plasma membrane under gravistimulation (Figures 5I and 5J). In consistent, these mutations disrupted the functions of LAZY4 in complementing the gravitropic defects of *lazy234* mutants (Figure 5K). Together, these data demonstrated that phosphorylation of LAZY4 by the MAPK cascade is important for its function in gravitropism.

Phosphorylation of LAZY4 promotes its interaction with TOC proteins on the surface of amyloplasts

Previous studies showed that mutating genes encoding TOC34, TOC75, TOC120 and TOC132, components of the Translocon of Outer Membrane of Chloroplasts (TOC) complexes, locating on the surface of both chloroplasts and amyloplasts, enhanced the gravitropic defects of *arg1*[36,37]. Thus, these TOC proteins played positive roles in gravitropism, but the underlying mechanism was unclear. Since LAZY proteins also localize on the surface of amyloplasts (Figures 2 and 3), and the phosphorylation of LAZY4 was induced by gravistimulation (Figure 5), we examined the possible interactions between LAZY4 and TOC proteins and studied whether phosphorylation affected the interactions. Among the 13 phosphorylation sites, we assayed all of them by gradually mutating them to Ala (A) or Asp (D), i.e. LAZY4-A5/D5, the 5 Ser/Thr sites located in the phosphorylated peptide in domain I; LAZY4-A9/D9, the 9 sites located in domain I and III; and LAZY4-A13/D13, all 13 sites mutated (detailed in Table S1). Using the yeast two-hybrid assay, we found that LAZY4 and phosphodead LAZY4 (A5, A9 and A13) did not interact with any TOC proteins (Figures 6A, S6A, S6B and Table S1). In contrast, one phosphomimic LAZY4 variant (LAZY4-D9) interacted strongly with TOC34, TOC120 and TOC132, all of which are receptors on the outer membrane of plastids and usually used for importing non-photosynthetic preproteins (Figures 6A, S6A, S6B and Table S1). Previous study showed that a TOC132 variant without N-terminus that only retains the GTP-binding and membrane domains (TOC132GM) could restore the gravitropic response of *arg1 toc132* to that of *arg1* single mutant[37]. We found that all three phosphomimic LAZY4 variants

(LAZY4-D5, LAZY4-D9, and LAZY4-D13) showed strong interaction with TOC132GM (Figures 6A, S6A, S6B, and Table S1). In contrast, the central pore component TOC75 did not interact with these phosphomimic LAZY4 proteins. Since LAZY4-D9 showed the strongest interaction with TOC proteins among the LAZY4 variants, it was selected to be transformed into the *lazy234* mutant for examination of localization and results showed a high co-localization pattern with TOC132-RFP around the amyloplasts in the columella cells (Figures 6B and 6C). These data suggest that phosphorylation of LAZY4 proteins enhances their interaction with the TOC proteins facing the cytosol, which may promote the translocation of LAZY4 proteins onto the surface of amyloplasts.

TOC proteins are essential for amyloplast localization and polar redistribution of LAZY4 proteins

To analyze the physiological significance of the interaction between phosphorylated LAZY4 and TOC proteins, we mutated *TOC120* and *TOC132* simultaneously with CRISPR/Cas9 in LAZY4-D9-GFP/*lazy234* and LAZY4-GFP/*lazy234* since these two *TOC* genes showed redundancy in chlorophyll synthesis (Figure S6A) [38,39]. The strong association of LAZY4-D9 with the amyloplast was disrupted by mutations in *TOC120* and *TOC132* (Figures 6D and S6C), indicating that the localization of LAZY4 on amyloplasts is dependent on TOC120 and TOC132. Gravistimulation-induced polar redistribution of LAZY4-D9 was disrupted in this $toc120^{CR}$ $toc132^{CR}$ mutant background (Figures 6D and 6F). Consistently, mutation of *TOC120* and *TOC132* disrupted the localization of LAZY4-GFP proteins onto the amyloplasts and their polar redistribution on the plasma membrane (Figures 6E, 6F, and S6C). Both materials with *toc120* and *toc132* mutations showed strong gravitropic defects (Figures 6G–6J). Thus, these TOC proteins are the key anchor proteins on the surface of amyloplasts that bind and facilitate the redistribution of LAZY proteins that are required for asymmetric root growth in plant gravitropic responses.

DISCUSSION

Gravity sensing, signal transduction, and differential growth are three sequential processes in plant gravitropism[2,5]. The starch-statolith hypothesis is the most widely-accepted theory explaining gravity sensing and is considered a dogma in the field of plant gravitropism[5–9,51], but the underlying molecular effects of amyloplast sedimentation are unknown. Here, we revealed that the molecular effect of amyloplast sedimentation is to promote the redistribution of LAZY proteins via the TOC proteins on the amyloplast surface. Based on this and previous studies, we suggest the following model for gravity sensing in plants (Figure 7): (i) During regularly vertical growth, amyloplasts settle to the bottom in root columella cells, and more LAZY proteins accumulate on the lower side of the plasma membrane. (ii) When plants tilt relative to the direction of gravity vector, gravistimulation induces the interaction between MKK5-MPK3 kinases and LAZY, resulting in increased phosphorylation of LAZY proteins. (iii) Phosphorylated LAZY proteins show stronger interactions with TOC34/120/132 proteins on the surface of amyloplasts, which may promote their translocation from the plasma membrane to the amyloplasts. (iv) Amyloplast sedimentation brings and guides the LAZY proteins toward the new lower side of columella cells. In this process, LAZY proteins may keep on trafficking between the amyloplasts

and adjacent plasma membrane. When the amyloplasts approach the new bottom, LAZY proteins are translocated from the surface of amyloplasts to the new lower side of the plasma membrane, re-establishing their polarity to promote asymmetric distribution of auxin and bending growth. (v) When the roots resume vertical growth, the LAZY proteins are dephosphorylated by unknown mechanisms, returning to their original state. Although the underlying mechanism of gravistimulation-triggered interaction between MPK3 and LAZY4 still need further investigation, the phosphorylation status of LAZY4 and its interaction with MPK3 can be regarded as two molecular indicators of plant responses to gravistimulation (Figure 5), which must be very useful in future studies in this field. Polarized LAZYs may regulate the asymmetric distribution of auxin through RLD and PIN proteins to mediate differential growth[33]. Since LAZY orthologs are prevalent and have also been demonstrated to regulate gravitropism in many other plant species, including rice[3,21–23], maize[20,24], *Medicago truncatula*[28], *Prunus domestica*[26] and *Lotus japonicus*[29], and TOC proteins are conserved in plant kingdom[38–41], it is possible that the mechanism revealed in this study is also applicable to other plants.

For the starch-statolith hypothesis, two models have been proposed to explain how the physical stimulus of amyloplast sedimentation is transformed into a biochemical signal responsible for the gravitropic curvature in plants[52]. One model postulates that sedimenting statoliths may activate mechano-sensitive ion channels via exerting a pressure on sensitive membranes or cytoskeletons within the statocyte cells[53,54], but no such plant mechanosensitive ion channel has been identified. Another model proposes that the contact of statoliths with membrane-bound receptors rather than pressure or tension exerted by the weight of statoliths may achieve graviperception[55], but the information about the receptor is unavailable. Our study proposes a model solely involving organelle movement that triggers the repolarization of the key gravitropism regulator LAZYs (Figure 7), suggesting that the molecular effect of amyloplast sedimentation probably doesn't need mechano-sensitive ion channels or receptors as proposed in the previous models. Interestingly, although the classical function of TOC proteins is to import proteins into plastids[38–41], it seems that relocation of LAZYs does not require them to be imported into amyloplasts (Figures 2, 3, 5 and 6). This unconventional working mechanism of TOCs makes repolarization of LAZYs simple and fast, resulting in a rapid gravitropic response. Since both movement of organelles and polarity formation are common phenomena, by revealing that the movement of a specific organelle directly triggers the protein re-polarity within cells, our study may also inspire other studies related to polarity.

Limitations of the study

Although our study provides critical insights into the molecular mechanism for the starch-statolith hypothesis, there are a few open issues. First, the underlying mechanism of gravistimulation-triggered interaction between MKK5-MPK3 and LAZY proteins needs further studies. What are the earliest signaling events after gravistimulation and whether MAPKKKs and/or other signaling molecules participate in this process remain the most exciting and challenging questions in the field. Second, we clearly showed that phosphorylation of LAZY4 increased its interaction with TOC proteins, and mutating TOCs disrupted the localization of LAZY4 onto amyloplasts, resulting in severe gravitropic

defects. Mutating the 13 phosphorylation sites within LAZY4 leads to obvious gravitropic defects, but the defects are not as severe as *lazy* null mutant or *toc120*^{CR} *toc132*^{CR} mutants. It is possible that more phosphorylation sites than we identified are involved in the interactions between LAZY and TOC proteins *in vivo*. Alternatively, there may exist other uncharacterized mechanisms besides phosphorylation that also contribute to the interaction. Third, the detailed trafficking processes of LAZY proteins between amyloplasts and the plasma membrane need future investigation. For example, how LAZY proteins are unloaded from amyloplasts and how the MAPK-mediated phosphorylation events crosstalk with the RLD-mediated cellular processes to ensure the changes of LAZY polarization in gravitropism.

STAR METHODS

RESOURCE AVAILABILITY

Lead contact—Further information and requests for resources and reagents should be directed to and will be fulfilled by the lead contact, Haodong Chen (chenhaodong@tsinghua.edu.cn)

Materials availability—Constructs and plant seeds generated in this study will be available from the lead contact upon request.

Data and code availability

- The mass spectrometry proteomics data have been deposited to the ProteomeXchange Consortium via the PRIDE partner repository with the dataset identifier PXD045213.
- This paper does not report original code.
- Any additional information required to reanalyze the data reported in this paper is available from the lead contact upon request.

EXPERIMENTAL MODEL AND STUDY PARTICIPANT DETAILS

Plant materials and growth conditions—All wild-type plants used in this study were the Columbia ecotype (Col) of *Arabidopsis thaliana*. Several mutants and transgenic lines used in this study were described previously: *pgm1*[13,14], *mpk6*$^{-/-}$ *mpk3RNAi*-est line[45], *pMPK3-MPK3-GFP*[45] and *DR5rev::GFP*[48,56]. Generation of plant materials was described in the method details.

The seeds were surface-sterilized by soaking in 15% (v/v) NaClO for around 10 min and washing in sterile distilled water for at least three times. After surface-sterilization, the seeds were plated on MS medium (4.4 g/L MS, 1% (w/v) sucrose, 0.8–1% (w/v) agar, pH 5.8), and cold-treated at 4 °C for 2 to 3 days in the dark. The seedlings were grown under continuous white light (70 μmol m^{-2} s^{-1}) or dark conditions as described in the figure legends. For growing in the dark, the plated seeds were illuminated under white light (70 μmol m^{-2} s^{-1}) for 6 h to induce germination before dark incubation. *Arabidopsis* seedlings were grown at

22 °C in a growth chamber. Adult *Arabidopsis* plants were grown under a 16 h/8 h day/night photoperiod at 22 °C.

METHOD DETAILS

Generation of mutants and transgenic plants—For mutating *Arabidopsis LAZY2*, *LAZY3*, and *LAZY4* simultaneously, we generated a modified Cas9 vector named as pEC-Cas9. First, rbcS-E9 terminator was cloned from pHEE401E[57], and inserted between the *Bam*H I and *Eco*R I sites of p35S-Cas9-SK[58] to replace the Nos terminator, resulting in p35S-Cas9-rbcS-E9t. Second, p35S-Cas9-rbcS-E9t was further modified by deleting a *Xho* I site upstream of the double CaMV 35S promoter and adding a *Nhe* I site between *Sal* I and *Hin*d III to generate p35S-Cas9-rbcS-E9t-M. Third, Ec1.2enEc1.1 promoter was cloned from pHEE401E[57] and inserted between *Nhe* I and *Xho* I sites to generate pEc1.2enEc1.1p-Cas9-rbcS-E9t (*abbr.*: pEC-Cas9). Two sgRNAs were designed for each *LAZY* gene (*LAZY2, LAZY3,* and *LAZY4*), and were inserted into the *Bbs* I sites of the pAtU6-26-M[59]. The primers used for annealing are listed in Table S5. The expression cassettes of six sgRNAs were digested with *Kpn* I and *Sal* I and ligated into pEC-Cas9. Then, the Cas9 cassettes were subcloned into the *Kpn* I and *Eco*R I sites of pCAMBIA1300 (Hyg) and pJIM19 (Gent) vectors to generate pCAMBIA1300-LAZY2/3/4 sgRNA and pJIM19-LAZY2/3/4 sgRNA. These binary constructs were transformed into wild type and *DR5rev::GFP* to generate *lazy2 lazy3 lazy4* (*lazy234*) and *DR5rev::GFP/lazy234* mutant lines. The mutants were analyzed using the primers listed in Table S5, and the lines *lazy234-1*, *lazy234-2*, *lazy234-3*, and *DR5rev::GFP/lazy234* were obtained.

To construct LAZY-GFP transgenic lines driven by the native promoter, we amplified the genomic DNAs of *LAZY2*, *LAZY3* and *LAZY4* including promoter regions by the primers listed in Table S5. Genomic fragments of *LAZY2*, *LAZY3* and *LAZY4* fused with GFP at the C-terminus were inserted into the *Sbf*I*/Xba* I, *Sbf*I*/Xho* I and *Sbf*I*/Spe* I sites of the plant binary vector pJIM19 (Bar) to construct pJIM19-LAZY2-GFP, pJIM19-LAZY3-GFP and pJIM19-LAZY4-GFP. Then, these LAZY-GFP constructs were transformed into wild type (Col) and *lazy234* respectively, and transgenic plants were selected with glufosinate ammonium (20 μg/mL). The obtained plants include *ProLAZY2:LAZY2-GFP* (*abbr.*: LAZY2-GFP/Col, only used in lateral roots fluorescence analysis in Figures S3F and S3G), *ProLAZY2:LAZY2-GFP/lazy234* (*abbr.*: LAZY2-GFP*/lazy234* or LAZY2-GFP), *ProLAZY3:LAZY3-GFP/lazy234* (*abbr.*: LAZY3-GFP*/lazy234* or LAZY3-GFP), and *ProLAZY4:LAZY4-GFP/lazy234* (*abbr.*: LAZY4-GFP*/lazy234* or LAZY4-GFP). These transgenic lines were crossed with *pgm1* to generate LAZY2-GFP*/lazy234 pgm1* (*abbr.*: LAZY2-GFP*/pgm1*), LAZY3-GFP*/lazy234 pgm1* (*abbr.*: LAZY3-GFP*/pgm1*) and LAZY4-GFP*/lazy234 pgm1* (*abbr.*: LAZY4-GFP*/pgm1*). LAZY4-GFP*/lazy234* was crossed with *mpk6*$^{-/-}$ *mpk3RNAi*-est line to generate LAZY4-GFP*/lazy23 mpk6*$^{-/-}$ *mpk3RNAi*-est (*abbr.*: LAZY4-GFP*/mpk6*$^{-/-}$ *mpk3RNAi*-est).

To construct GFP-fused truncated LAZY driven by the *LAZY* native promoter, we amplified the promoter and truncated coding sequences of *LAZY* using the primers listed in Table S5. The LAZY2ΔN and LAZY4ΔN related fragments were inserted into pCAMBIA1300 (Hyg), and LAZY3ΔN related fragments were inserted into pJIM19

(Bar). Then, these constructs were transformed into *lazy234* triple mutants. Transgenic plants were selected with hygromycin B (50 μg/mL) or glufosinate ammonium (20 μg/mL). The obtained plants include *ProLAZY2:LAZY2ΔN-GFP/lazy234* (*abbr.*: LAZY2ΔN-GFP/*lazy234*), *ProLAZY3:LAZY3ΔN-GFP/lazy234* (*abbr.*: LAZY3ΔN-GFP/*lazy234*), and *ProLAZY4:LAZY4ΔN-GFP/lazy234* (*abbr.*: LAZY4ΔN-GFP/*lazy234*).

To construct *ProLAZY4:LAZY4-D9-GFP/lazy234* and *ProLAZY4:LAZY4-A13-GFP/lazy234* transgenic plants, we amplified the promoter and coding sequences of *LAZY4* from wild type plants using the primers listed in Table S5. Point mutations were generated by overlap PCR and the mutation sites are listed in Table S1. Then, the fragments with GFP were inserted into pJIM19 (Bar), and transformed into *lazy234* triple mutants. Transgenic plants were selected with glufosinate ammonium (20 μg/mL). The obtained plants include *ProLAZY4:LAZY4-D9-GFP/lazy234* (*abbr.*: LAZY4-D9-GFP/*lazy234*) and *ProLAZY4:LAZY4-A13-GFP/lazy234* (*abbr.*: LAZY4-A13-GFP/*lazy234*).

To construct LAZY4-GFP/*lazy234 toc120*^{CR} *toc132*^{CR} and LAZY4-D9-GFP/*lazy234 toc120*^{CR} *toc132*^{CR}, we designed two sgRNAs for each *TOC* (*TOC120* and *TOC132*), and were inserted into the *Bbs* I sites of the pAtU6-26-M[56] vector. The primers used for annealing are listed in Table S5. The expression cassettes of four sgRNAs were digested with *Kpn* I and *Sal* I and inserted into the *Kpn* I and *Eco*R I sites of pUBQ10:Cas9-P2A-GFP (Gent) [59] vector. This construct was transformed into LAZY4-GFP*/lazy234* and LAZY4-D9-GFP/*lazy234* transgenic lines. The mutants were analyzed using the primers listed in Table S5.

To construct TOC132-RFP/LAZY4-D9-GFP/*lazy234* transgenic lines, we amplified the genomic DNAs of *TOC132* including promoter regions and coding sequences by the primers listed in Table S5. Genomic fragments of TOC132 were inserted into the *Sal* I and *Bam*H I sites of the plant binary vector *pCAMBIA1300(Hyg)-mRFP*. Then, the *pCAMBIA1300(Hyg)-TOC132-mRFP* construct was transformed into LAZY4-D9-GFP/*lazy234* transgenic lines, and transgenic plants were selected with hygromycin B (50 μg/mL).

Gravitropic phenotype analyses—In experiments studying gravitropism of primary roots under regular growth, seedlings were grown 4 days on vertically-oriented MS plates under white light or darkness. In experiments studying the tropic responses of primary roots after gravistimulation, seedlings were grown vertically under white light for around 4 days, and then the plates were re-orientated 90°. In experiments studying growth orientations of lateral roots (LR), seedlings were grown vertically on MS plates under white light. Then, the primary roots were aligned to the gravity vector on the 7th day, and the plants continued to grow for several additional days. Root growth angles were measured by Image J software[60]. The distribution frequency of root growth angles was plotted using the R statistics program (http://www.rproject.org).

Microscopic observation and analyses—For fluorescence observation of *Arabidopsis* seedlings under vertical growth or gravistimulation, the fluorescent images were collected using the confocal laser scanning microscope (Zeiss LSM800) or spinning-disk confocal

microscopy (Andor Dragonfly 200) with a vertical objective table. 488 nm laser was used to detect the fluorescence of LAZY-GFP (including mutated variants), and 561 nm laser was used to detect FM4-64 or TOC132-RFP. Differential interference contrast microscopy (DIC) was used to collect the images of the amyloplasts. Around four-day-old seedlings grown under white light were used for fluorescence observation unless specified otherwise.

Signal intensity was calculated by ImageJ[60]. Signal intensity ratios of LAZY-GFP proteins in columella cells after gravistimulation were calculated by comparing the fluorescence of the lower outer and upper outer lateral plasma membranes of central columella cells or lateral columella cells (the columella cells adjacent to central columella cells). The mean gray value of several regions of interest was calculated as the background, and subtracted from the signal intensity of the images acquired by spinning-disk confocal microscopy. Signal ratio for one root was calculated as an average of signal intensity ratios within this root[61]. The details of signal intensity ratio analysis are shown in Figures S3D and S3E.

Immuno-electron microscopy—The roots of LAZY4-GFP/*lazy234* seedlings were fixed by high-pressure freezing (HPF, Leica EM HPM100) with 5% sucrose as a cryoprotectant. The freeze-substitution solution was 0.4% (w/v) uranyl acetate in acetone, and the freeze-substitution was carried out as follows. First, the samples were kept at −90 °C for 48 hours, and then the temperature was slowly raised to −50 °C in 20 hours. Then, the samples were rinsed in ethanol for three times in two hours. Second, the temperature was slowly raised to −35 °C and kept for 48 hours, and then the solution was changed to Lowicryl HM20 resin (Electron Microscopy Sciences, 14340) with gradually increasing concentration (50%, 75%, 100% v/v in ethanol). The samples in pure resin were raised to room temperature, and the resin was changed for another three times. Third, the resin was polymerized with UV at −35 °C for 48 h in a Leica AFS apparatus. Resin blocks with samples were cut into 80-nm ultrathin sections and mounted on nickel grids with a single slot, and blocked with PBS containing 0.5% BSA-c (Aurion, 900.022) and 0.05% Tween for 10 min. GFP antibody (1:10, Abcam, ab290) diluted in blocking solution was added on each cover sheet, and kept for 30 min at room temperature. Then, the sections were washed 5 times with PBS (2 min for each wash), and labeled with protein A Gold 10 nm (1:50; Dept. of Cell Biology, UMC Utrecht, the Netherlands) for 30 min at room temperature. After several washes with PBS, the sections were fixed in 1% (w/v) glutaraldehyde, washed with distilled water and counterstained with 2% uranyl acetate solution. The sections on grids were imaged at 80 kV in a JEOL JEM-1400 Flash (HC) TEM using a CMOS camera (XAROSA, EMSIS).

Protein-lipid overlay assay—Recombinant GST-tagged proteins were expressed and purified using E.coli Transetta (DE3). Strips with 15 different phospholipids on a nitrocellulose membrane were blocked in blocking buffer (3% w/v BSA in PBST) at 4 °C overnight. Then, 0.5 μg/mL GST-tagged proteins in blocking buffer were incubated with the membranes for 1 h at room temperature. The membranes were washed three times with PBST, and then incubated with anti-GST (1:2000 in blocking buffer) for 1 h at room temperature. Further, the membranes were washed three times with PBST, and then

incubated with second antibody (1:8000 in blocking buffer) for 1 h at room temperature. Chemiluminescence were detected using GE Healthcare Amersham ECL kit.

Immunoprecipitation-Mass Spectrometry (IP-MS)—The following buffers were prepared for carrying out IP-MS on LAZY4-GFP and MPK3-GFP. Lysis buffer: 1x RIPA buffer (Abcam: ab156034), 1 mM PMSF, 1x protease inhibitor cocktail (Mei5bio: MF182-plus-01), and 1x phosphatase inhibitor cocktail (Mei5bio: MF183-01). Dilution buffer: 50 mM Tris-HCl (pH 7.5), 1 mM Beta-glycerophosphate, 1 mM Sodium orthovanadate, 0.5% (w/v) Sodium deoxycholate, 1mM EGTA, 1mM EDTA, and 150 mM Sodium chloride. Wash buffer: 100 mM Tris-HCl (pH 7.5), 10 mM EDTA, 10 mM EGTA, and 5 mM KCl. Four-day-old *Arabidopsis* seedlings (around 4 g) were collected and ground into powder with liquid nitrogen, and proteins were extracted using lysis buffer and diluted to around 1 mg/mL with dilution buffer. Immunoprecipitation was then performed with GFP-Trap beads (ChromoTek, gtma-20), using 50 μL GFP-Trap beads for around 6 mg proteins. The proteins were eluted from the beads with 50–60 μL 0.2 M glycine solution (pH 2.5) by gently shaking for 30–60 s, followed by magnetic or centrifuging separation. Then, the supernatant was transferred into another empty centrifuge tube and 10% (v/v) Tris-base (pH 10.4) was added into the tube.

The protein samples were analyzed on an Orbitrap Fusion Lumos Tribrid Mass Spectrometer (Thermo). After dithiothreitol reduction and iodoacetamide alkylation, the proteins were digested with trypsin (Sequencing grade modified; Promega) overnight at 37 °C. The resulting tryptic peptides were desalted with C18 tips (Pierce #87784) and dried in a vacuum centrifuge concentrator. The peptides were resolved using 0.1% formic acid and loaded onto a trap column (Acclaim PepMap™ 100 75 μm × 2 cm nanoViper, C18, 3 μm, 100Å, Thermo) connecting to an analytical column (Acclaim PepMap™ RSLC 75 μm × 15 cm nanoViper, C18, 2 μm, 100Å, Thermo) on a nanoflow HPLC Easy-nLC 1200 system (Thermo Fisher Scientific), using a 75 min LC gradient at 280 nL/min. Buffer A is consisted of 0.1% (v/v) formic acid in H_2O and Buffer B is consisted of 0.1% (v/v) formic acid in 80% acetonitrile. The gradient was set as follows: 4%–8% B in 5 min; 8%–20% B in 45 min; 20%–30% B in 10 min; 30%–90% B in 13 min; 90% B in 2 min. Proteomic analyses were performed on a Thermo Orbitrap Fusion Lumos mass spectrometer (Thermo Fisher Scientific) using a nano-electrospray ion source with electrospray voltages of 2.2 kV. Data-dependent acquisition was performed using Xcalibur software in profile spectrum data type. The MS1 full scan was set at a resolution of 120,000 @ m/z 200, AGC target 5e5 and maximum IT 90 ms by orbitrap mass analyzer (300–1500 m/z), followed by MS2 scans generated by HCD fragmentation at a resolution of 30,000 @ m/z 200, AGC target 5e4. The fixed first mass of MS2 spectrum was set as 110.0 m/z. Isolation window was set as 1.6 m/z. The normalized collision energy (NCE) was set as NCE 30%.

The MS spectrometry data were analyzed by software Proteome Discoverer or Maxquant. The phosphorylation sites of LAZY4 or MPK3 were identified based on MS2 results. MS1 area intensities of phosphorylated peptides were calculated for quantification, normalized by the total area intensity of phosphorylated and non-phosphorylated peptides. For analyzing the phosphorylation ratio of MPK3 Co-Immunoprecipitated by LAZY4-GFP, two replicates

detecting the peptide containing the key phosphorylation sites T196/Y198 at GS 0.5 h from the time series experiments were used, and the third replicate was carried out additionally.

GST pull-down—Recombinant proteins were expressed and purified using E.coli Transetta (DE3). Recombinant His-tagged MPK3 (~10 μg) was activated by incubation with recombinant His-MKK5^{DD} (~1 μg, mutated MKK5 with constitutive activity) in the presence of 50 μM ATP in 50 μL of reaction buffer (25 mM Tris, pH 7.5, 10 mM $MgCl_2$ and 1mM DTT) at 37 °C for 30 min. These proteins were mixed with GST-LAZY4ΔCCL (~100 μg) at 4 °C overnight, and then incubated with Glutathione Sepharose 4B (GE Healthcare) for 3 h at 4 °C. Alternatively, these proteins were mixed with GST-LAZY4ΔCCL and incubated with Glutathione Sepharose 4B (GE Healthcare) at 4 °C overnight. Resins were washed three times with wash buffer (First, 50 mM Tris-HCl pH 7.5, 150 mM NaCl; Second, 50 mM Tris-HCl pH 7.5, 200 mM NaCl; Third, 50 mM Tris-HCl pH 7.5, 250 mM NaCl). Pellet proteins were analyzed by Western blot using anti-His and anti-GST antibodies.

***In vitro* kinase assay—**Recombinant proteins were expressed and purified using E.coli Transetta (DE3). Recombinant GST-tagged MPK3 (10 μg) was activated by incubation with recombinant GST-MKK5^{DD} (1 μg) in the presence of 50 μM ATP in 50 μL of reaction buffer (25 mM Tris, pH 7.5, 10 mM $MgCl_2$ and 1mM DTT) at 37 °C for 30 min. Then, GST-LAZY4ΔCCL (~100 μg) was added and reacted in the same reaction buffer with 10 mM ATP at 37 °C for 60 min. Equal volumes of 2x SDS loading buffer were added and boiled at 95 °C for 10 min to stop the reaction. Phosphorylation of LAZY4 proteins was analyzed by mass-spectrometry and Western blot.

Antibody generation—We generated a polyclonal LAZY4 antibody designated anti-LAZY4. The synthetic peptide KQEITHRPSISSASSHHPR derived from the *Arabidopsis* LAZY4 was injected into rabbits as antigen, using 400 μg for the first injection and 200 μg for the following three times. Polyclonal anti-LAZY4 antibodies were purified from rabbit serum using the synthetic peptide by affinity chromatography.

Yeast two hybrid assays—The yeast two-hybrid assays were performed as described previously[62]. The coding sequences of TOC33, TOC34, TOC64, TOC75 (TOC75-III), TOC90, TOC120, TOC132, TOC132-GM, TOC159-GM, LAZY4, LAZY4-D5/9/13 and LAZY4-A5/9/13 were amplified using the primers listed in Table S5, and the mutation sites are listed in Table S1. The TOC fragments were subcloned into the pLexA vector, and LAZY4, LAZY4- D5/9/13 and LAZY4- A5/9/13 were subcloned into the pB42AD vector. The LexA fusion constructs (bait) and the activation domain fusion constructs (prey) were co-transformed into yeast strain EGY48[p8op-lacZ] (CLONTECH). Clones containing both constructs were selected on medium lacking His, Trp and Ura, and transferred onto minimal SD/Gal/Raf/-His-Trp-Ura agar plates containing X-gal for testing β-Galactosidase activity[63].

QUANTIFICATION AND STATISTICAL ANALYSIS

Root tip angles and fluorescence intensity were measured using ImageJ (https://imagej.net/software/fiji/). MS1 intensity was evaluated by

Proteome Discoverer (Thermo Fisher Scientific, https://www.thermofisher.cn/cn/zh/home/industrial/mass-spectrometry/liquid-chromatography-mass-spectrometry-lc-ms/lc-ms-software/multi-omics-data-analysis/proteome-discoverer-software.html). Student's t-test was performed in comparison of two independent groups. For multiple comparison, one-way ANOVA with post-hoc Tukey's HSD test or Dunnett's t-test was performed using IBM SPSS software (https://www.ibm.com/spss). The distribution of root tips was evaluated by Kolmogorov-Smirnov test with Bonferroni correction. The statistical details, including the statistical tests used and exact value of n for each measurement, were presented in figure legends and figures. The significant differences were indicated as following: ***, $P < 0.001$; **, $P < 0.01$; *, $P < 0.05$; ns, not significant, $P > 0.05$.

Supplementary Material

Refer to Web version on PubMed Central for supplementary material.

ACKNOWLEDGMENTS

We thank Prof. Tongda Xu for *mpk6*$^{-/-}$*mpk3RNAi*-est and *pMPK3-MPK3-GFP* seeds, Profs. Jian-Kang Zhu and Qijun Chen for CRISPR/Cas9 plasmids, Profs. Li-Jia Qu, Tongda Xu, William Terzaghi, Genji Qin, Li Yu, Guangshuo Ou, Yule Liu, Yijun Qi, Shanjin Huang, Daoxin Xie and Haiteng Deng for helpful comments, and Huifang Qin and Jingxi Sun for technical assistance. We thank the National Center for Protein Sciences and Core Facilities of Life Sciences at Peking University in Beijing, China, particularly Dr. Dong Liu and Dr. Qi Zhang for assistance with the mass spectrometry experiments, and Dr. Yiqun Liu, Dr. Yingchun Hu, and Miss. Pengyuan Dong for assistance with ImmunoEM. We thank the Protein Chemistry and Proteomics Facility at Tsinghua University particularly Dr. Yuling Chen for assistance with the mass spectrometry experiments. We thank Cryo-EM Facility of China National Center for Protein Sciences (Beijing) at Tsinghua University particularly Dr. Ying Li for assistance with HPF and immunolabeling. This study was supported by the National Natural Science Foundation of China (32022005, 31621001, 32170287), Tsinghua University Dushi Program (20231080035), and the Tsinghua-Peking Center for Life Sciences. J.D. was funded by grants from the National Institute of Health (GM1851907) and the National Science Foundation (2049642).

INCLUSION AND DIVERSITY

We support inclusive, diverse, and equitable conduct of research.

REFERENCES

1. Knight T (1806). On the direction of the radicle and germen during the vegetation of seeds. Philos. Trans. R. Soc. Lond. Ser. B 96, 99–108. 10.1098/rstl.1806.0006.
2. Vandenbrink JP, and Kiss JZ (2019). Plant responses to gravity. Semin. Cell Dev. Biol. 92, 122–125. 10.1016/j.semcdb.2019.03.011. [PubMed: 30935972]
3. Uga Y, Sugimoto K, Ogawa S, Rane J, Ishitani M, Hara N, Kitomi Y, Inukai Y, Ono K, Kanno N, et al. (2013). Control of root system architecture by DEEPER ROOTING 1 increases rice yield under drought conditions. Nat. Genet. 45, 1097–1102. 10.1038/ng.2725. [PubMed: 23913002]
4. Huang G, Liang W, Sturrock CJ, Pandey BK, Giri J, Mairhofer S, Wang D, Muller L, Tan H, York LM, et al. (2018). Rice actin binding protein RMD controls crown root angle in response to external phosphate. Nat Commun 9, 2346. 10.1038/s41467-018-04710-x. [PubMed: 29892032]
5. Morita MT (2010). Directional gravity sensing in gravitropism. Annu. Rev. Plant Biol. 61, 705–720. 10.1146/annurev.arplant.043008.092042. [PubMed: 19152486]
6. Chin S, and Blancaflor EB (2022). Plant Gravitropism: From Mechanistic Insights into Plant Function on Earth to Plants Colonizing Other Worlds. Methods Mol Biol 2368, 1–41. 10.1007/978-1-0716-1677-2_1. [PubMed: 34647245]

7. Nemec B (1900). Uber die Art der Wahrnehmung des Schwerkraftreizes bei den Pflanzen. Ber. Deut. Bot. Ges. 18, 241–245. 10.1111/J.1438-8677.1900.TB04905.X.
8. Darwin F (1903). The statolith theory of geotropism. Nature 67, 571–572. 10.1038/067571a0.
9. Haberlandt G (1900). Ueber die Perception des geotropischen Reizes. Ber. Deut. Bot. Ges. 18, 261–272. 10.1111/j.1438-8677.1900.tb04908.x.
10. Blancaflor EB, Fasano JM, and Gilroy S (1998). Mapping the functional roles of cap cells in the response of Arabidopsis primary roots to gravity. Plant Physiol. 116, 213–222. 10.1104/pp.116.1.213. [PubMed: 9449842]
11. Fukaki H, Wysocka-Diller J, Kato T, Fujisawa H, Benfey PN, and Tasaka M (1998). Genetic evidence that the endodermis is essential for shoot gravitropism in Arabidopsis thaliana. Plant J. 14, 425–430. 10.1046/j.1365-313x.1998.00137.x. [PubMed: 9670559]
12. Tsugeki R, and Fedoroff NV (1999). Genetic ablation of root cap cells in Arabidopsis. Proc Natl Acad Sci U S A 96, 12941–12946. 10.1073/pnas.96.22.12941. [PubMed: 10536027]
13. Caspar T, and Pickard BG (1989). Gravitropism in a starchless mutant of Arabidopsis : Implications for the starch-statolith theory of gravity sensing. Planta 177, 185–197. 10.1007/BF00392807.
14. Kiss JZ, Hertel R, and Sack FD (1989). Amyloplasts are necessary for full gravitropic sensitivity in roots of Arabidopsis thaliana. Planta 177, 198–206. 10.1007/BF00392808.
15. Zheng Z, Zou J, Li H, Xue S, Wang Y, and Le J (2015). Microrheological insights into the dynamics of amyloplasts in root gravity-sensing cells. Mol Plant 8, 660–663. 10.1016/j.molp.2014.12.021. [PubMed: 25704165]
16. Went FW, and Thimann KV (1937). Phytohormones (New York: The macmillan company). 10.5962/bhl.title.5695.
17. Friml J, Wisniewska J, Benkova E, Mendgen K, and Palme K (2002). Lateral relocation of auxin efflux regulator PIN3 mediates tropism in Arabidopsis. Nature 415, 806–809. 10.1038/415806a. [PubMed: 11845211]
18. Kleine-Vehn J, Ding Z, Jones AR, Tasaka M, Morita MT, and Friml J (2010). Gravity-induced PIN transcytosis for polarization of auxin fluxes in gravity-sensing root cells. Proc Natl Acad Sci U S A 107, 22344–22349. 10.1073/pnas.1013145107. [PubMed: 21135243]
19. Jenkins MT, and Gerhardt F (1931). A gene influencing the composition of the culm in maize. Iowa Ag Exp Sta Research Bull 11, 121–151. https://dr.lib.iastate.edu/handle/20.500.12876/62445.
20. Van Overbeek J (1936). “Lazy,” an A-geotropic form of maize: “Gravitational indifference” rather than structural weakness accounts for prostrate growth-habit of this form. J Heredity 27, 93–96. 10.1093/oxfordjournals.jhered.a104191.
21. Jones JW, and Adair CR (1938). A “lazy” mutation in rice. J Heredity 29, 315–318. 10.1093/oxfordjournals.jhered.a104527.
22. Li P, Wang Y, Qian Q, Fu Z, Wang M, Zeng D, Li B, Wang X, and Li J (2007). LAZY1 controls rice shoot gravitropism through regulating polar auxin transport. Cell Res. 17, 402–410. 10.1038/cr.2007.38. [PubMed: 17468779]
23. Yoshihara T, and Iino M (2007). Identification of the gravitropism-related rice gene LAZY1 and elucidation of LAZY1-dependent and -independent gravity signaling pathways. Plant Cell Physiol. 48, 678–688. 10.1093/pcp/pcm042. [PubMed: 17412736]
24. Dong Z, Jiang C, Chen X, Zhang T, Ding L, Song W, Luo H, Lai J, Chen H, Liu R, et al. (2013). Maize LAZY1 mediates shoot gravitropism and inflorescence development through regulating auxin transport, auxin signaling, and light response. Plant Physiol. 163, 1306–1322. 10.1104/pp.113.227314. [PubMed: 24089437]
25. Yoshihara T, Spalding EP, and Iino M (2013). AtLAZY1 is a signaling component required for gravitropism of the Arabidopsis thaliana inflorescence. Plant J. 74, 267–279. 10.1111/tpj.12118. [PubMed: 23331961]
26. Guseman JM, Webb K, Srinivasan C, and Dardick C (2017). DRO1 influences root system architecture in Arabidopsis and Prunus species. Plant J. 89, 1093–1105. 10.1111/tpj.13470. [PubMed: 28029738]

27. Che X, Splitt BL, Eckholm MT, Miller ND, and Spalding EP (2023). BRXL4-LAZY1 interaction at the plasma membrane controls Arabidopsis branch angle and gravitropism. Plant J. 113, 211–224. 10.1111/tpj.16055. [PubMed: 36478485]

28. Ge L, and Chen R (2016). Negative gravitropism in plant roots. Nat Plants 2, 16155. 10.1038/nplants.2016.155. [PubMed: 27748769]

29. Chen Y, Xu S, Tian L, Liu L, Huang M, Xu X, Song G, Wu P, Sato S, Jiang H, and Wu G (2020). LAZY3 plays a pivotal role in positive root gravitropism in Lotus japonicus. J. Exp. Bot. 71, 168–177. 10.1093/jxb/erz429. [PubMed: 31559427]

30. Taniguchi M, Furutani M, Nishimura T, Nakamura M, Fushita T, Iijima K, Baba K, Tanaka H, Toyota M, Tasaka M, and Morita MT (2017). The Arabidopsis LAZY1 Family Plays a Key Role in Gravity Signaling within Statocytes and in Branch Angle Control of Roots and Shoots. Plant Cell 29, 1984–1999. 10.1105/tpc.16.00575. [PubMed: 28765510]

31. Yoshihara T, and Spalding EP (2017). LAZY Genes Mediate the Effects of Gravity on Auxin Gradients and Plant Architecture. Plant Physiol. 175, 959–969. 10.1104/pp.17.00942. [PubMed: 28821594]

32. Yang P, Wen Q, Yu R, Han X, Deng XW, and Chen H (2020). Light modulates the gravitropic responses through organ-specific PIFs and HY5 regulation of LAZY4 expression in Arabidopsis. Proc Natl Acad Sci U S A 117, 18840–18848. 10.1073/pnas.2005871117. [PubMed: 32690706]

33. Furutani M, Hirano Y, Nishimura T, Nakamura M, Taniguchi M, Suzuki K, Oshida R, Kondo C, Sun S, Kato K, et al. (2020). Polar recruitment of RLD by LAZY1-like protein during gravity signaling in root branch angle control. Nat Commun 11, 76. 10.1038/s41467-019-13729-7. [PubMed: 31900388]

34. Waite JM, Collum TD, and Dardick C (2020). AtDRO1 is nuclear localized in root tips under native conditions and impacts auxin localization. Plant Mol. Biol. 103, 197–210. 10.1007/s11103-020-00984-2. [PubMed: 32130643]

35. Sedbrook JC, Chen R, and Masson PH (1999). ARG1 (altered response to gravity) encodes a DnaJ-like protein that potentially interacts with the cytoskeleton. Proc Natl Acad Sci U S A 96, 1140–1145. 10.1073/pnas.96.3.1140. [PubMed: 9927707]

36. Stanga JP, Boonsirichai K, Sedbrook JC, Otegui MS, and Masson PH (2009). A role for the TOC complex in Arabidopsis root gravitropism. Plant Physiol. 149, 1896–1905. 10.1104/pp.109.135301. [PubMed: 19211693]

37. Strohm AK, Barrett-Wilt GA, and Masson PH (2014). A functional TOC complex contributes to gravity signal transduction in Arabidopsis. Front Plant Sci 5, 148. 10.3389/fpls.2014.00148. [PubMed: 24795735]

38. Andres C, Agne B, and Kessler F (2010). The TOC complex: preprotein gateway to the chloroplast. Biochim Biophys Acta 1803, 715–723. 10.1016/j.bbamcr.2010.03.004. [PubMed: 20226817]

39. Kubis S, Patel R, Combe J, Bedard J, Kovacheva S, Lilley K, Biehl A, Leister D, Rios G, Koncz C, and Jarvis P (2004). Functional specialization amongst the Arabidopsis Toc159 family of chloroplast protein import receptors. Plant Cell 16, 2059–2077. 10.1105/tpc.104.023309. [PubMed: 15273297]

40. Jin Z, Wan L, Zhang Y, Li X, Cao Y, Liu H, Fan S, Cao D, Wang Z, Li X, et al. (2022). Structure of a TOC-TIC supercomplex spanning two chloroplast envelope membranes. Cell 185, 4788–4800 e4713. 10.1016/j.cell.2022.10.030. [PubMed: 36413996]

41. Liu H, Li A, Rochaix JD, and Liu Z (2023). Architecture of chloroplast TOC-TIC translocon supercomplex. Nature. 10.1038/s41586-023-05744-y.

42. Xu J, and Zhang S (2015). Mitogen-activated protein kinase cascades in signaling plant growth and development. Trends Plant Sci. 20, 56–64. 10.1016/j.tplants.2014.10.001. [PubMed: 25457109]

43. Wang H, Ngwenyama N, Liu Y, Walker JC, and Zhang S (2007). Stomatal development and patterning are regulated by environmentally responsive mitogen-activated protein kinases in Arabidopsis. Plant Cell 19, 63–73. 10.1105/tpc.106.048298. [PubMed: 17259259]

44. Meng X, Wang H, He Y, Liu Y, Walker JC, Torii KU, and Zhang S (2012). A MAPK cascade downstream of ERECTA receptor-like protein kinase regulates Arabidopsis inflorescence

architecture by promoting localized cell proliferation. Plant Cell 24, 4948–4960. 10.1105/tpc.112.104695. [PubMed: 23263767]

45. Huang R, Zheng R, He J, Zhou Z, Wang J, Xiong Y, and Xu T (2019). Noncanonical auxin signaling regulates cell division pattern during lateral root development. Proc Natl Acad Sci U S A 116, 21285–21290. 10.1073/pnas.1910916116. [PubMed: 31570617]
46. Jia W, Li B, Li S, Liang Y, Wu X, Ma M, Wang J, Gao J, Cai Y, Zhang Y, et al. (2016). Mitogen-Activated Protein Kinase Cascade MKK7-MPK6 Plays Important Roles in Plant Development and Regulates Shoot Branching by Phosphorylating PIN1 in Arabidopsis. PLoS Biol. 14, e1002550. 10.1371/journal.pbio.1002550. [PubMed: 27618482]
47. Ottenschlager I, Wolff P, Wolverton C, Bhalerao RP, Sandberg G, Ishikawa H, Evans M, and Palme K (2003). Gravity-regulated differential auxin transport from columella to lateral root cap cells. Proc Natl Acad Sci U S A 100, 2987–2991. 10.1073/pnas.0437936100. [PubMed: 12594336]
48. Ulmasov T, Murfett J, Hagen G, and Guilfoyle TJ (1997). Aux/IAA proteins repress expression of reporter genes containing natural and highly active synthetic auxin response elements. Plant Cell 9, 1963–1971. 10.1105/tpc.9.11.1963. [PubMed: 9401121]
49. Bailey MJ, and Prehoda KE (2015). Establishment of Par-Polarized Cortical Domains via Phosphoregulated Membrane Motifs. Dev. Cell 35, 199–210. 10.1016/j.devcel.2015.09.016. [PubMed: 26481050]
50. Brzeska H, Guag J, Remmert K, Chacko S, and Korn ED (2010). An experimentally based computer search identifies unstructured membrane-binding sites in proteins: application to class I myosins, PAKS, and CARMIL. J. Biol. Chem. 285, 5738–5747. 10.1074/jbc.M109.066910. [PubMed: 20018884]
51. Su SH, Keith MA, and Masson PH (2020). Gravity Signaling in Flowering Plant Roots. Plants (Basel) 9. 10.3390/plants9101290.
52. Su SH, Gibbs NM, Jancewicz AL, and Masson PH (2017). Molecular Mechanisms of Root Gravitropism. Curr. Biol. 27, R964–R972. 10.1016/j.cub.2017.07.015. [PubMed: 28898669]
53. Leitz G, Kang BH, Schoenwaelder ME, and Staehelin LA (2009). Statolith sedimentation kinetics and force transduction to the cortical endoplasmic reticulum in gravity-sensing Arabidopsis columella cells. Plant Cell 21, 843–860. 10.1105/tpc.108.065052. [PubMed: 19276442]
54. Perbal G, and Driss-Ecole D (2003). Mechanotransduction in gravisensing cells. Trends Plant Sci. 8, 498–504. 10.1016/j.tplants.2003.09.005. [PubMed: 14557047]
55. Limbach C, Hauslage J, Schafer C, and Braun M (2005). How to activate a plant gravireceptor. Early mechanisms of gravity sensing studied in characean rhizoids during parabolic flights. Plant Physiol. 139, 1030–1040. 10.1104/pp.105.068106. [PubMed: 16183834]
56. Zadnikova P, Petrasek J, Marhavy P, Raz V, Vandenbussche F, Ding Z, Schwarzerova K, Morita MT, Tasaka M, Hejatko J, et al. (2010). Role of PIN-mediated auxin efflux in apical hook development of Arabidopsis thaliana. Development 137, 607–617. 10.1242/dev.041277. [PubMed: 20110326]
57. Wang ZP, Xing HL, Dong L, Zhang HY, Han CY, Wang XC, and Chen QJ (2015). Egg cell-specific promoter-controlled CRISPR/Cas9 efficiently generates homozygous mutants for multiple target genes in Arabidopsis in a single generation. Genome Biol 16, 144. 10.1186/s13059-015-0715-0. [PubMed: 26193878]
58. Feng Z, Zhang B, Ding W, Liu X, Yang DL, Wei P, Cao F, Zhu S, Zhang F, Mao Y, and Zhu JK (2013). Efficient genome editing in plants using a CRISPR/Cas system. Cell Res. 23, 1229–1232. 10.1038/cr.2013.114. [PubMed: 23958582]
59. Wang J, and Chen H (2020). A novel CRISPR/Cas9 system for efficiently generating Cas9-free multiplex mutants in Arabidopsis. aBIOTECH 1, 6–14. 10.1007/s42994-019-00011-z. [PubMed: 36305009]
60. Schneider CA, Rasband WS, and Eliceiri KW (2012). NIH Image to ImageJ: 25 years of image analysis. Nat. Methods 9, 671–675. 10.1038/nmeth.2089. [PubMed: 22930834]
61. Grones P, Abas M, Hajny J, Jones A, Waidmann S, Kleine-Vehn J, and Friml J (2018). PID/WAG-mediated phosphorylation of the Arabidopsis PIN3 auxin transporter mediates polarity switches during gravitropism. Sci Rep 8, 10279. 10.1038/s41598-018-28188-1. [PubMed: 29980705]

62. Serino G, Tsuge T, Kwok S, Matsui M, Wei N, and Deng XW (1999). Arabidopsis cop8 and fus4 mutations define the same gene that encodes subunit 4 of the COP9 signalosome. Plant Cell 11, 1967–1980. 10.1105/tpc.11.10.1967. [PubMed: 10521526]

63. Dong J, Tang D, Gao Z, Yu R, Li K, He H, Terzaghi W, Deng XW, and Chen H (2014). Arabidopsis DE-ETIOLATED1 represses photomorphogenesis by positively regulating phytochrome-interacting factors in the dark. Plant Cell 26, 3630–3645. 10.1105/tpc.114.130666. [PubMed: 25248553]

Highlights

- Gravistimulation triggers MAPK-mediated phosphorylation of LAZY proteins
- Phosphorylation increases LAZY's interaction with TOCs on the surface of amyloplasts
- Amyloplast sedimentation carries LAZY proteins to the new bottom of columella cells
- LAZY translocates from amyloplasts to adjacent plasma membrane to form new polarity

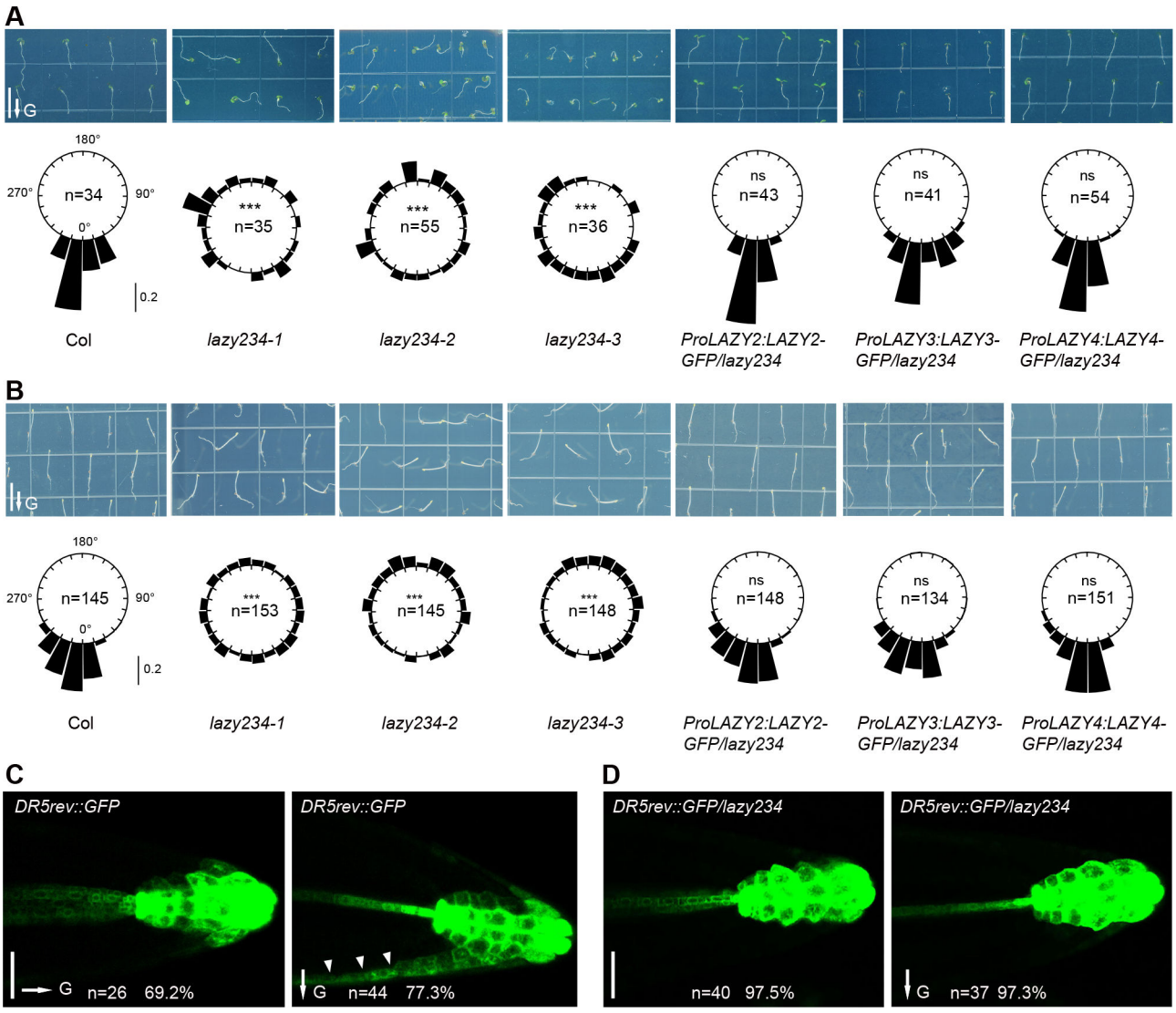

Figure 1. *Arabidopsis* lacking *LAZY2, 3* and *4* lose the gravitropic response and gravistimulation-induced auxin redistribution in roots.

(A and **B)** Col, *lazy234* triple mutants, and complementation lines were grown vertically under white light for 4 days (A) or in the dark for 3 days (B). Upper, representative seedlings. Scale bars, 1 cm. Lower, frequencies of root tip angles in each 15° division around a circle, and the bars indicate relative frequency. Root tip distribution was compared with Col, and significant differences were evaluated by the Kolmogorov-Smirnov test with Bonferroni correction (***, $P < 0.001$; ns, not significant, $P > 0.05$).

(**C** and **D**) Expression of *DR5rev::GFP* in wild-type and *lazy234* primary roots before (left) and after gravistimulation via 90° reorientation (right) for around 4 hours. Random primary roots of *DR5rev::GFP/ lazy234* were aligned to the gravity vector before the reorientation, therefore no gravity vector was marked in D, left. Scale bars, 50 μm. Arrowheads indicate the asymmetric accumulation of auxin on one side.

In A to D, arrows labeled “G” indicate the direction of gravity.

See also Figures S1, and S2.

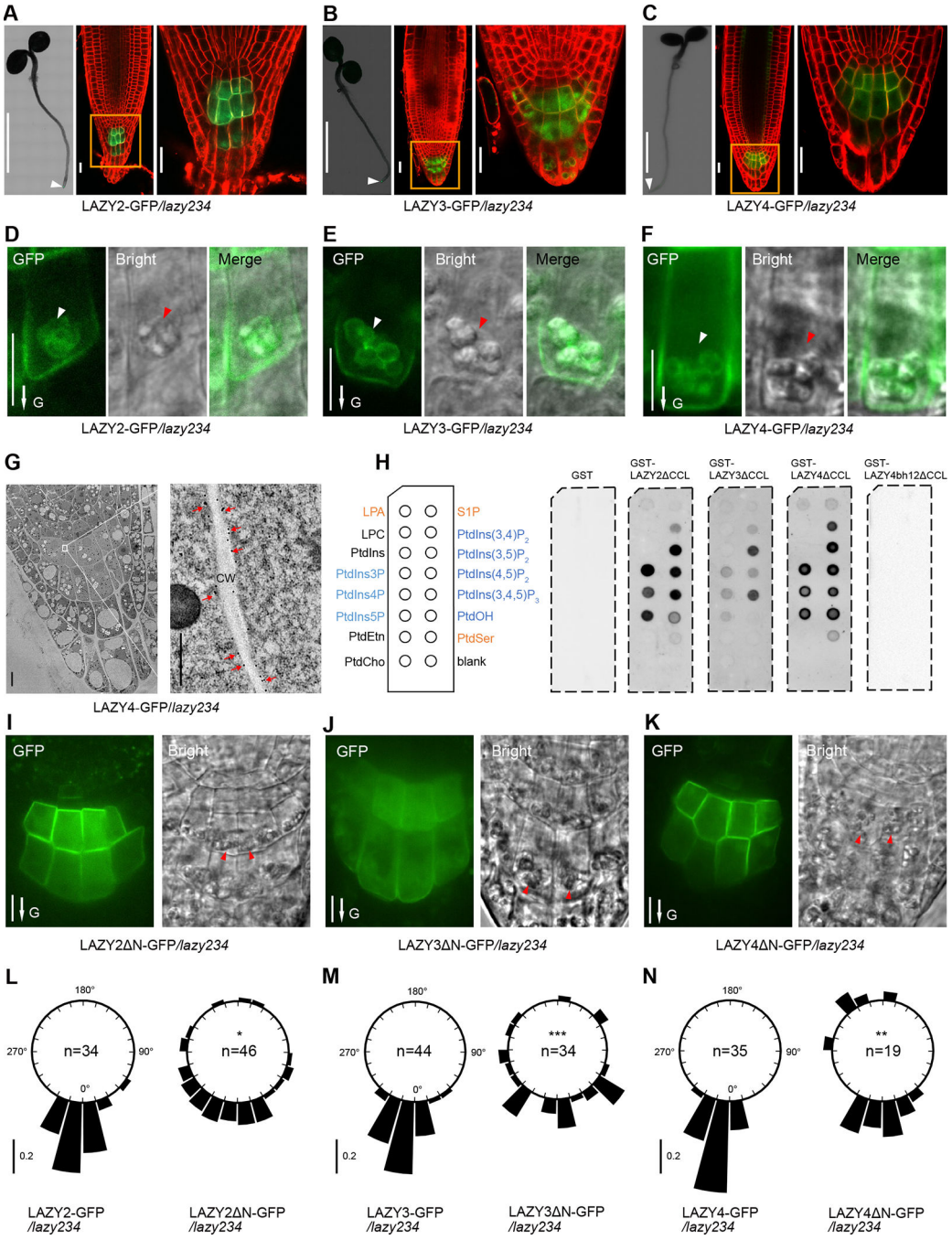

Figure 2. *Arabidopsis* LAZY2, 3 and 4 proteins are predominantly localized on the amyloplasts and plasma membrane of columella cells in roots.

(A to **C)** Localization of GFP-tagged LAZY2, LAZY3, and LAZY4 proteins (green) at the root tip of seedlings grown in white light. For each figure panel, left, a confocal image (assembled) shows the predominant expression of LAZY-GFP at the root tip (white arrowhead); middle, a confocal image shows the subcellular localization of LAZY-GFP with an enlarged view (right). Cell outlines were stained with 5 μM FM4-64 for 2 minutes (red).

Scale bars, 0.2 cm (left); 20 μm (middle and right). A, B and C are representative images of roots of 10, 8 and 13 seedlings, respectively.

(**D** to **F**) Detailed localization of LAZY2/3/4-GFP protein (green) at the plasma membrane and around the amyloplast envelope in columella cells. White and red arrowheads point to the amyloplasts observed under the Confocal or DIC microscopy, respectively. Scale bars, 10 μm. D, E and F are representative images of roots of 15, 17 and 12 seedlings, respectively. For LAZY4-GFP in F, an image with a relatively strong appearance of amyloplast localization was selected for improved visualization of intracellular signals.

(G) Tracking LAZY4-GFP localization by immuno-gold labeling. The root tips of 4-day-old light-grown LAZY4-GFP/*lazy234* seedlings were analyzed by immuno-electron microscopy using GFP antibody. Red arrows indicate the gold particles on the plasma membranes. CW, Cell Wall. Scale bars, 5 μm (left); 0.5 μm (right).

(H) Protein-lipid overlay assay with purified GST, GST-LAZY2ΔCCL, GST-LAZY3ΔCCL, GST-LAZY4ΔCCL and GST-LAZY4bh12ΔCCL using PBS buffer. LPA, lysophosphatidic acid; S1P, sphingosine-1-phosphate; LPC, lysophosphatidylcholine; PtdIns, phosphatidylinositol; PtdIns(x)$P_{(y)}$, mono/bis/tris phosphates, x is the phosphorylation position while y is the number of the phosphate groups; PtdEtn, phosphatidyl-ethanolamine; PtdCho, phosphatidylcholine; PtdOH, phosphatidic acid; PtdSer, phosphatidylserine. LAZY4bh12 means mutating K/R to A within two BH peaks (details in Figure S3C). ΔCCL means the deletion of the last 14 amino acids, which made these LAZY proteins express better in E.coli. Equal amounts of GST or GST-tagged proteins (2.5 μg) were used for each membrane. Anti-GST was used for the immunoblot.

(I to **K)** Localization of LAZY2ΔN-GFP, LAZY3ΔN-GFP, LAZY4ΔN-GFP proteins at the root tip of seedlings grown in white light. ΔN indicates the deletion of N terminus of LAZY proteins (details in methods). Red arrowheads indicate the amyloplasts observed under the DIC microscopy. Scale bars, 10 μm. I, J and K are representative images of roots of 16, 12 and 20 seedlings, respectively.

(**L** to **N**) Full length and N-terminal deletion LAZY2/3/4-GFP/*lazy234* transgenic lines were grown vertically under white light for 4 days. Frequencies of root tip angles in each 15° division around a circle are shown, and the bar indicates relative frequency. Root tip distribution of truncated LAZY2/3/4-GFP/*lazy234* transgenic lines was compared with full length lines, and significant differences were evaluated by Kolmogorov-Smirnov test with Bonferroni correction (***, $P < 0.001$; **, $P < 0.01$; *, $P < 0.05$).

In D to F, I to K, arrows labeled “G” indicate the direction of gravity.

See also Figure S3.

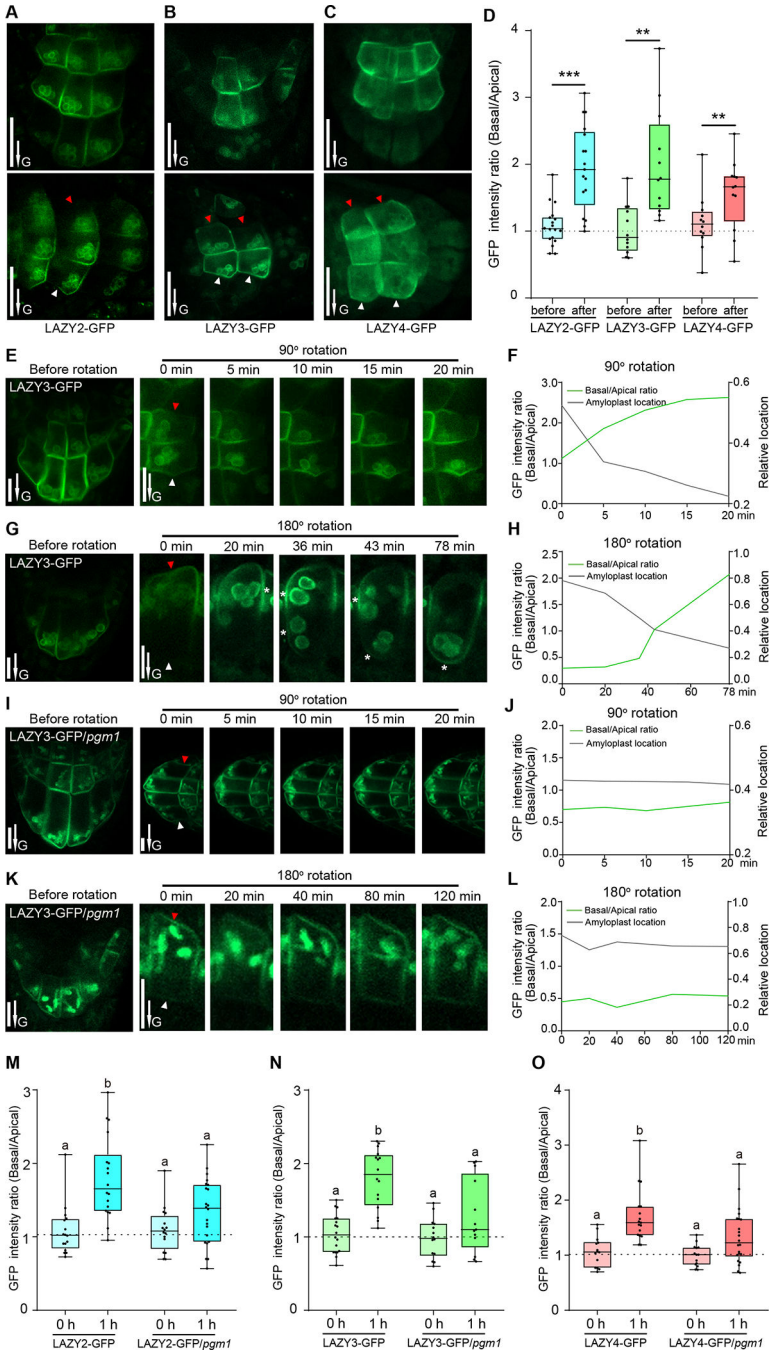

Figure 3. Amyloplast sedimentation promotes the gravity-triggered redistribution of LAZY proteins to the lower side of columella cells.

(**A** to **D**) LAZY proteins show polar distribution in columella cells under the control of gravity. (A to C) Seedlings were grown vertically on MS plates, and reoriented 90° and kept for 0.5 to 1 h of gravistimulation. Red and white arrowheads indicate the accumulation of LAZY-GFP proteins on the upper and lower sides of columella cells, respectively. Scale bars, 20 μm. (D) Statistical analysis of fluorescence intensity ratios of the two sides of columella cells (Basal/Apical) in panels A to C. Asterisks indicate Student's t-test values

(***, P < 0.001; **, P < 0.01; n = 18, 17, 12, 12, 12 and 12 respectively). The method for intensity ratio analysis is shown in Figures S3D and S3E.

(**E** to **H**) Gravity-triggered redistribution of LAZY proteins to the lower side of columella cells correlates with the sedimentation of amyloplasts. LAZY3-GFP seedlings were grown vertically and then reoriented 90° (E) or 180° (G), and fluorescence was collected at several time points. Red and white arrowheads indicate the upper and lower sides of columella cells, respectively. White stars in panel G indicate the positions of plasma membrane adjacent to amyloplasts, where the fluorescence is strong. Scale bars, 10 μm. The fluorescence intensity ratio (Basal/Apical) and average relative-locations of the amyloplasts (relative distances from the amyloplasts to the new bottoms of cells, cell heights were set as 1) are shown in F and H. E and G are representative images of 6 seedling roots for each rotation condition.

(**I** to **L**) Mutation of *PGM1* delayed both amyloplast sedimentation and redistribution of LAZY3-GFP proteins triggered by gravistimulation. Data collection and analyses were the same as in E to H. I and K are representative images of 3 seedling roots for each rotation condition.

(**M** to **O**) Mutation of *PGM1* delayed the redistribution of LAZY2, LAZY3 and LAZY4 proteins. The seedlings were grown vertically and then reoriented 90° and kept 1 h for gravistimulation. The statistical analyses of fluorescence intensity ratios of LAZY-GFP proteins on the two sides of columella cells (Basal/Apical) are shown. Significant differences in GFP intensity ratios were evaluated by one-way ANOVA with post-hoc Tukey's HSD test (alpha=0.05; M, n = 16, 18, 16 and 22 respectively; N, n = 18, 16, 14 and 13 respectively; O, n = 14, 17, 14 and 22 respectively). Representative images are shown in Figure S4B.

In A, B, C, E, G, I and K, arrows labeled "G" indicate the direction of gravity. In E, G, I, and K, the images labeled as "Before rotation" were rotated from the images labeled as "0 min" after 90° or 180° rotation, to show the original orientation.

See also Figures S3 and S4.

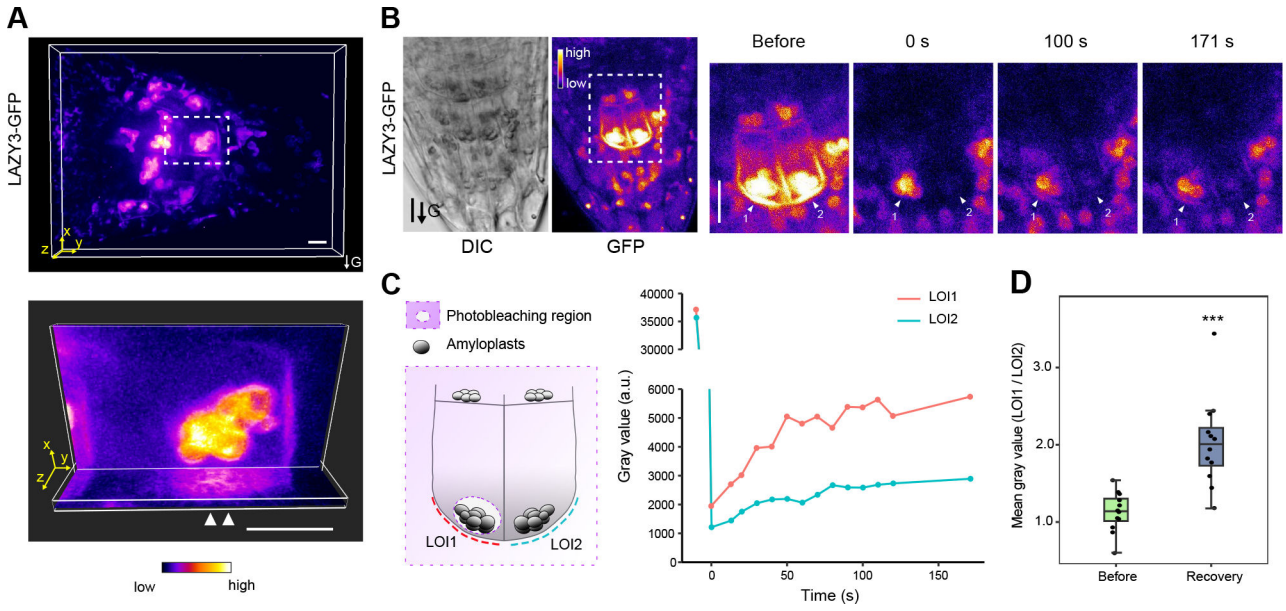

Figure 4. LAZY3 proteins translocate from the amyloplasts to the plasma membrane.

(A) 3-D reconstruction of the fluorescence of LAZY3-GFP in columella cells under gravistimulation. Seedlings of LAZY3-GFP/*lazy234* were grown vertically under white light for 4 days, and then rotated 90° to the horizontal position for gravistimulation for around 0.5 h. Images were acquired using a spinning-disk confocal microscope with a z-series taken every 0.25 μm for a range of 10.5 μm. Upper, representative 3-D view of confocal image stacks of columella cells expressing LAZY3-GFP. Lower, ortho slicer view of XY plane and YZ plane of the cell in white dashed box (upper), extended section of 2.0 μm is shown for each slicer. White arrow heads indicate the accumulated signal on the lower side of plasma membrane adjacent to the amyloplasts. 3-D views were generated by Imaris. Scale bars, 10 μm. This is a representative image of 13 seedling roots.

(B) Fluorescence of LAZY3-GFP on plasma membrane in columella cells in FRAP experiment. Left, representative images of roots expressing LAZY3-GFP; right, zoomed image of the region in white dashed box (left) at different time points showing fluorescence recovery. Arrows labeled with numbers indicate a symmetrical pair of columella cells with similar fluorescence before photobleaching. LAZY3-GFP was bleached by 488 nm laser in two labeled cells and adjacent cells except for the amyloplast region in cell #1. Bleached region is also diagrammed in (C). The fluorescence was collected immediately after photobleaching (0 s) and at indicated time after photobleaching. Scale bars, 10 μm. These are representative images of 12 seedling roots.

(C) Fluorescence recovery on plasma membrane of representative cells in (B). Left, diagram showing the bleached region. LOI, line of interest on which fluorescence signal intensity was measured. Right, the recovery rate of signal intensity of LOI1 and LOI2.

(D) Statistical analysis of signal intensity ratios of LOI1/LOI2 before bleaching and after recovery in different roots. Symmetric columella cells were selected for analysis as in (B). Intensity was measured on LOI1 and LOI2 after a recovery of 100 s (***, $P < 0.001$; n = 12).

See also Videos S1 and S2.

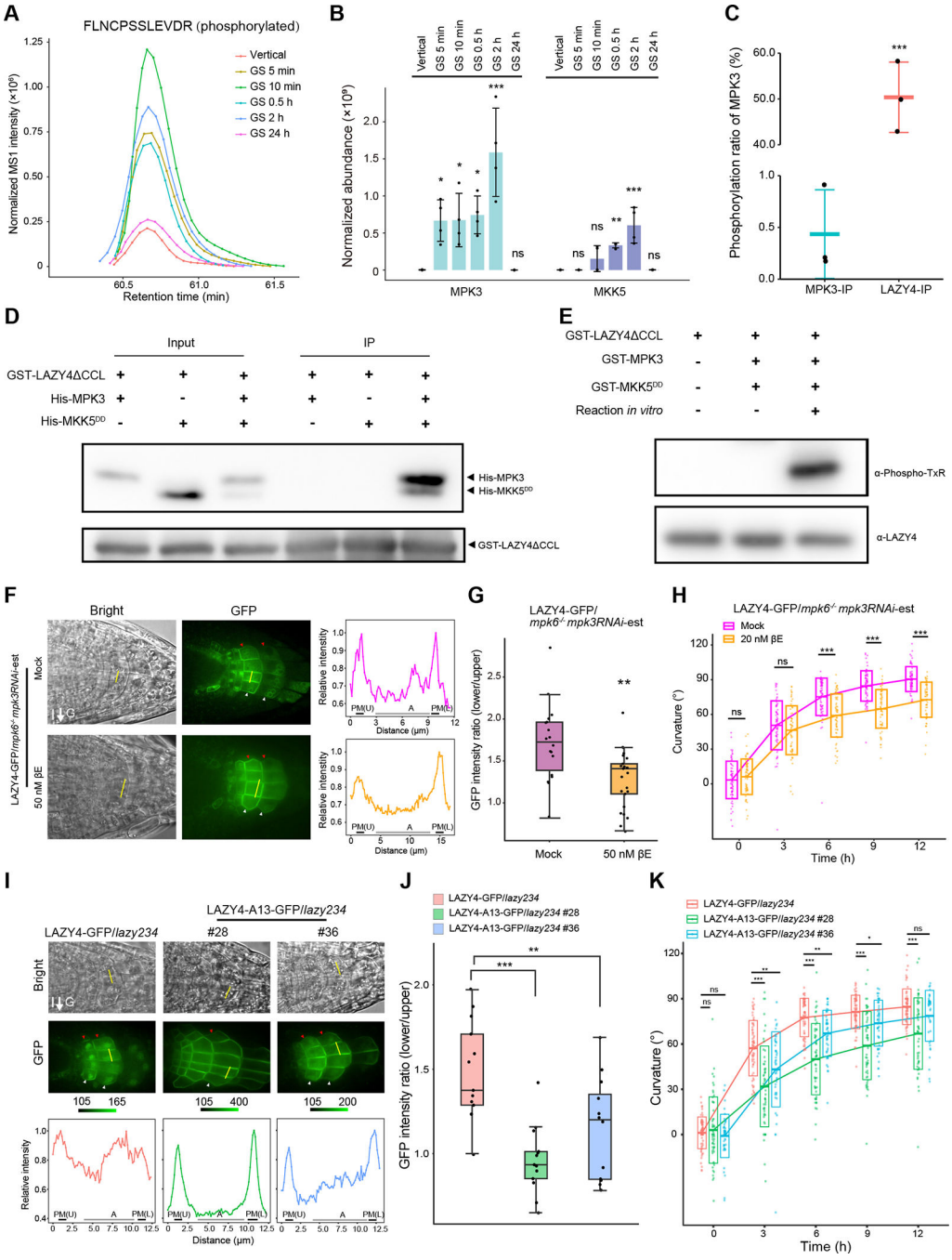

Figure 5. Gravity-induced phosphorylation of LAZY4 by MKK5-MPK3.

(A) Gravistimulation induces the phosphorylation of LAZY4. LAZY4-GFP seedlings were grown vertically or gravistimulated (90° reorientation) for 5 min, 10 min, 0.5 h, 2 h and 24 h. Then, LAZY4-GFP proteins were immunoprecipitated for Mass-Spectrometry (MS) analysis. The MS result was summarized in Figure S5 and Table S1, and the normalized abundance of the representative phosphopeptide “FLNCPSSLEVDR” (S139 and S140 sites) are shown. The result is a representative of four replicates.

(B) LAZY4 shows stronger interaction with MPK3 and MKK5 after gravistimulation in *Arabidopsis*. The original data is from the experiment in panel A, including four replicates. The barplot shows the comparison of MPK3 and MKK5 abundance co-immunoprecipitated by LAZY4-GFP (mean ± SD). MS1 abundance of all identified peptides of MPK3 and MKK5 in the MS results were summed and normalized using MS1 abundance of bait protein LAZY4-GFP. Protein abundance of MPK3 and MKK5 in different samples was compared with that in the vertical, and significant difference was evaluated by one-way ANOVA with post-hoc Dunnett's t-test (***, $P < 0.001$; **, $P < 0.01$; *, $P < 0.05$; $n = 4$).

(C) LAZY4 prefers to interact with phosphorylated MPK3 in *Arabidopsis*. MPK3-GFP and LAZY4-GFP seedlings were grown vertically and then gravistimulated (90° reorientation) for 0.5 h. The phosphorylation ratio of the MPK3 peptides containing T196/Y198 sites was calculated using the MS data of MPK3-GFP IP samples (MPK3-IP) and LAZY4-GFP Co-IP samples (LAZY4-IP). Data are represented as mean ± SD. Significant differences were evaluated by Student's t-test (***, $P < 0.001$; $n = 3$).

(D) LAZY4 interacts with MPK3 and MKK5 *in vitro*. Recombinant GST-LAZY4ΔCCL, His-MPK3 and His-MKK5^{DD} proteins purified from E.coli were incubated at 4 °C overnight. For lane 3, His-MPK3 and His-MKK5^{DD} was mixed and treated for 30 min at 37 °C with ATP, and then incubated with GST-LAZY4ΔCCL. Glutathione Sepharose 4B was used for immunoprecipitation. Pellet fractions were separated by SDS-PAGE, and visualized by anti-His and anti-GST immunoblots. GST-LAZY4ΔCCL was used since it is easier to express in E.coli than full length GST-LAZY4.

(E) MPK3 and MKK5 phosphorylate LAZY4 *in vitro*. The recombinant proteins were mixed and reacted as indicated. For *in vitro* reactions recombinant GST-MPK3 and GST-MKK5^{DD} proteins were mixed and treated for 30 min at 37 °C with ATP, and then GST-LAZY4ΔCCL was added and treated for 60 min under the same conditions. The proteins were resolved by SDS-PAGE, and visualized by anti-Phospho-TxR (recognizing the phosphorylation of T18 in LAZY4) and anti-LAZY4 immunoblots. The LAZY4 proteins were also analyzed by Mass-Spectrometry, and the phosphorylation sites are summarized in Table S1.

(**F** and **G**) Mutation of *MPK3* and *MPK6* disrupts the localization of LAZY4-GFP onto the surface of amyloplasts and polar redistribution of LAZY4-GFP on the plasma membrane. (F) LAZY4-GFP/*mpk6*$^{-/-}$*mpk3RNAi*-est seedlings were grown vertically on MS plates containing DMSO (Mock) or 50 nM β-estradiol (βE) to induce RNAi of *MPK3* expression for 3 days. The seedlings were transferred to MS plates containing 10 μM CHX to inhibit protein synthesis, and reoriented 90° for 0.5 to 1-h gravistimulation. Left and middle, representative confocal images of LAZY4-GFP; Right, fluorescence intensity profile along the yellow line marked in the representative cells. Max intensity in each profile was set to 1.0, and relative intensity was calculated for plots. PM (U), upper side of the plasma membrane; PM (L), lower side of the plasma membrane; A, amyloplasts. Red and white arrowheads indicate the accumulation of LAZY4-GFP proteins on the upper and lower sides of columella cells, respectively. (G) Statistical analysis of fluorescence intensity ratios of the two sides of columella cells (Basal/Apical) in panel F. Asterisks indicate Student's t-test values (**, $P < 0.05$; $n = 18$ and 24 respectively).

(**H**) Mutation of *MPK3* and *MPK6* delays the gravitropic responses of roots. LAZY4-GFP/*mpk6*$^{-/-}$*mpk3RNAi*-est seedlings were grown vertically under white light on MS plates

containing DMSO (Mock) or 20 nM βE to induce RNAi of *MPK3* expression. Seedlings were grown vertically for 4 days and reoriented 90° for gravistimulation. The crossbars indicate mean ± SD. At each time point, significant difference of root tip angles between mock group and treated group was evaluated by Student's t-test (***, $P < 0.001$; ns, not significant, $P > 0.05$; n = 72 and 65 respectively).

(I and **J)** Mutation of phosphorylation sites within LAZY4 disrupts the localization of LAZY4-GFP onto the surface of amyloplasts and polar redistribution of LAZY4-GFP on the plasma membrane. (I) Localization of *Arabidopsis* LAZY4-GFP and LAZY4-A13-GFP proteins in columella cells under gravistimulation for 0.5 to 1 h with CHX treatment. Upper and middle, representative confocal images of LAZY4-GFP and LAZY4-A13-GFP; Lower, fluorescence intensity profile along the yellow line marked in the representative cells. The method for profile analysis is the same as in panel F. Scale bars, 10 μm. Red and white arrowheads indicate the upper and lower sides of columella cells respectively. (J) Statistical analysis of fluorescence intensity ratios of the two sides of columella cells (Basal/Apical) in panel I. Fluorescence intensity ratios were compared with the first group, and significant difference was evaluated by one-way ANOVA with post-hoc Dunnett's t-test (***, $P < 0.001$; **, $P < 0.01$; n = 13, 13 and 12 respectively).

(K) Mutation of phosphorylation sites disrupts the gravitropic responses of roots. LAZY4-GFP/*lazy234* and LAZY4-A13-GFP/*lazy234* seedlings were grown vertically for 4 days, and then rotated 90° to the horizontal position for gravistimulation. The crossbars indicate mean ± SD. At each time point, root tip angles were compared with the first group, and significant difference was evaluated by one-way ANOVA with post-hoc Dunnett's t-test (***, $P < 0.001$; **, $P < 0.01$; ns, not significant, $P > 0.05$; n = 66, 55 and 48 respectively).

In F and I, arrows labeled "G" indicate the direction of gravity.

See also Figure S5, Tables S1, S2, S3 and S4.

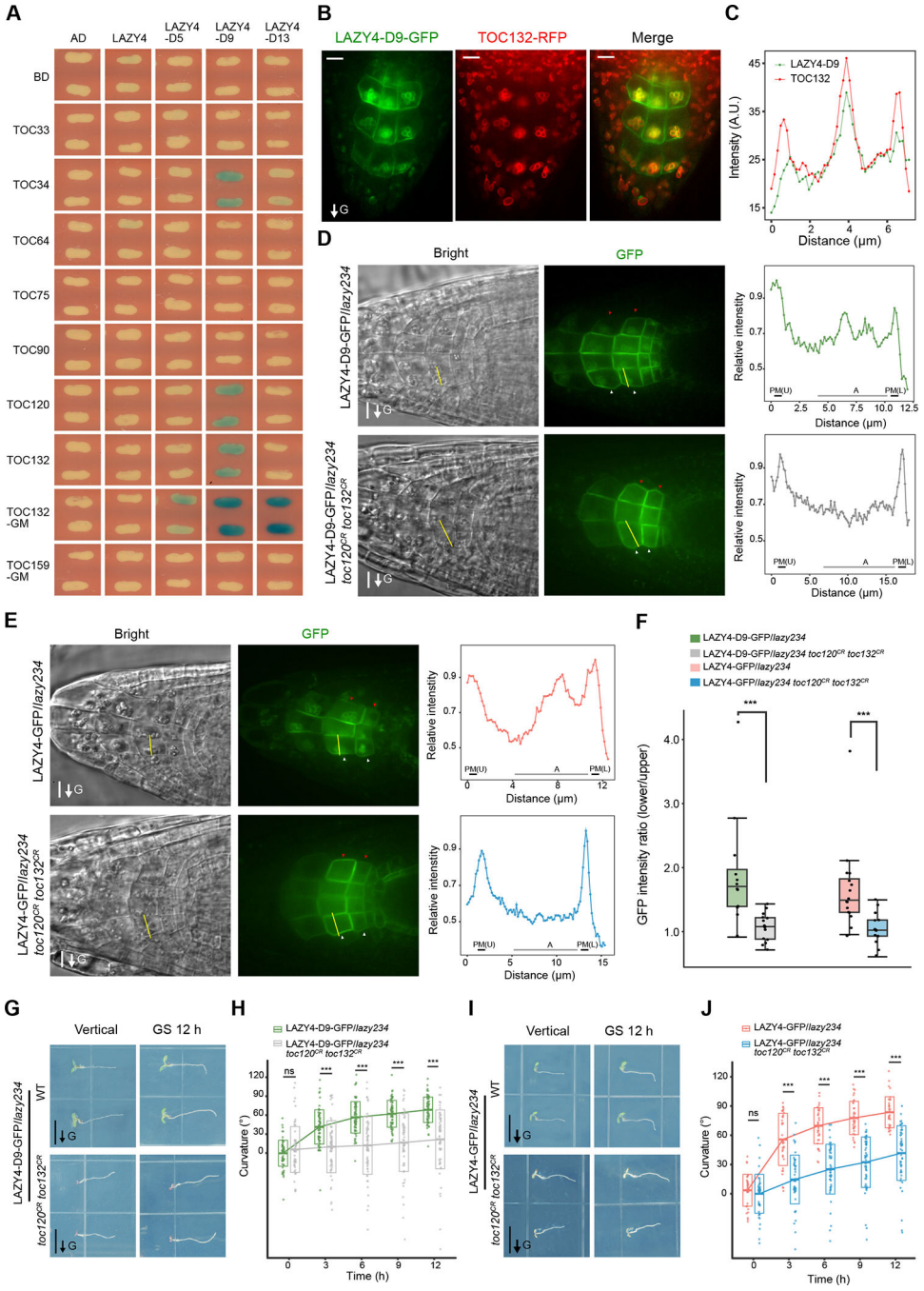

Figure 6. Phosphorylation of LAZY4 promotes its interaction with TOC proteins, which control the redistribution of LAZY4 and the gravitropic response.

(**A**) Yeast two-hybrid assays to test interactions between LAZY4 variants and TOC proteins. The phosphorylation sites of LAZY4 were mutated to Asp (D) as indicated in Table S1. Blue indicates positive interactions. Reporter: LacZ; substrate, X-Gal. TOC132GM and TOC159GM indicate the GTP-binding and membrane domains of these TOC proteins. The yeasts were grown for 24 h, and results from 40-h growth with more LAZY4 variants are shown in Figure S6B.

(B and **C)** Co-localization of LAZY4-D9-GFP and TOC132-RFP in root columella cells. (B) TOC132-RFP was transformed into LAZY4-D9-GFP/*lazy234*, and the seedlings were grown vertically on MS plates for 4 days. Root tip fluorescence was collected. Scale bars, 10 μm. (C) Statistical analysis of fluorescence intensities of LAZY4-D9-GFP and TOC132-RFP in columella cells. Green and red lines show the respective fluorescence intensities of GFP and RFP along the yellow dotted line marked in panel B. a.u., arbitrary units. These are representative images of roots of 20 seedlings.

(D to F) Mutation of *TOC120* and *TOC132* disrupts the localization of LAZY4 onto the surface of amyloplasts and polar redistribution of LAZY4 on the plasma membrane. (D) LAZY4-D9-GFP/*lazy234* and LAZY4-D9-GFP/*lazy234 toc120*^{CR} *toc132*^{CR} seedlings were grown vertically on MS plates for 4 days. The seedlings were transferred to other MS plates, and reoriented 90° for 0.5 to 1-h gravistimulation. Red and white arrowheads indicate the accumulation of LAZY-GFP proteins on the upper and lower sides of columella cells, respectively. Left and middle, representative confocal images of LAZY4-GFP; Right, fluorescence intensity profile along the yellow line marked in the representative cells. Max intensity in each profile was set to 1.0, and relative intensity was calculated for plots. Scale bars, 10 μm. PM (U), upper side of the plasma membrane; PM (L), lower side of the plasma membrane; A, amyloplasts. (E) LAZY4-GFP/*lazy234* and LAZY4-GFP/*lazy234 toc120*^{CR} *toc132*^{CR} seedlings were grown vertically on MS plates for 4 days. The seedlings were transferred to MS plates with 10 μM CHX to inhibit protein synthesis during the 0.5 to 1-h gravistimulation. The following experiments and analysis were the same as in panel D. Scale bars, 10 μm. (F) Statistical analysis of fluorescence intensity ratios of the two sides of columella cells (Basal/Apical) in panel D and E. Asterisks indicate Student's t-test values (***, $P < 0.001$; n = 13, 15, 16 and 14 respectively).

(G to **J)** Mutation of *TOC120* and *TOC132* disrupts the gravitropic responses of roots. Seedlings were grown vertically on MS plates for 4 days, and then rotated 90° to the horizontal position for gravistimulation. (G and I) Representative seedlings. Scale bars, 0.5 cm. (H and J) The crossbars indicate mean ± SD. At each time point, significant differences of root tip angles between two groups were evaluated by Student's t-test (***, $P < 0.001$; ns, not significant, $P > 0.05$; H, n = 71 and 65 respectively; J, n = 35 and 53 respectively). See also Figure S6, Table S1.

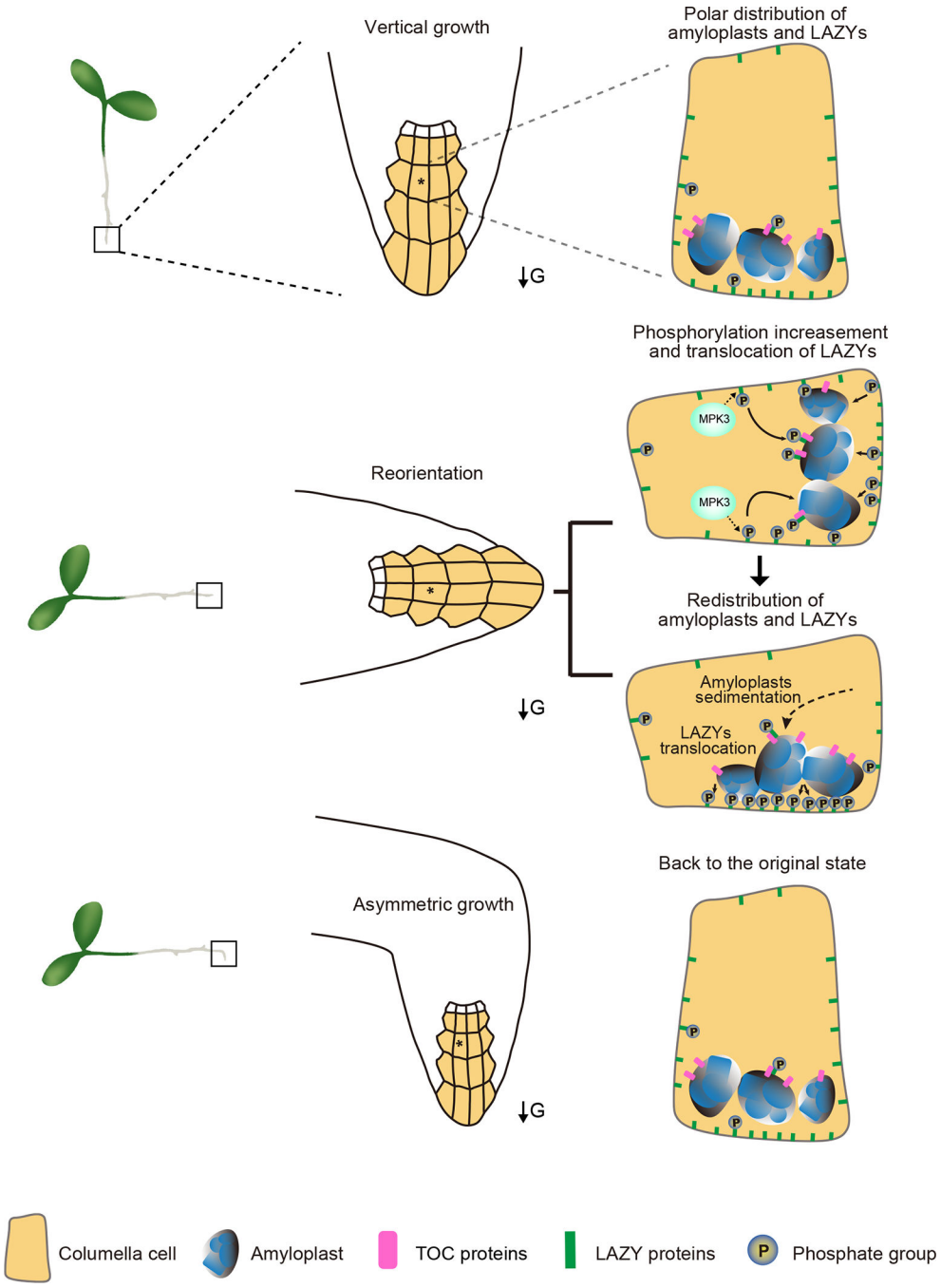

Figure 7. Model for gravity sensing in plant roots.

Under vertical growth, more LAZY proteins accumulate on the lower side of the plasma membrane in columella cells of roots. Gravistimulation via reorientation triggers the interactions between the MKK5-MPK3 kinase module and LAZY proteins, resulting in increased phosphorylation of LAZY proteins. Subsequently, phosphorylated LAZYs may translocate onto the surface of amyloplasts by directly interacting with TOC proteins. Amyloplast sedimentation guides the LAZY proteins to distribute onto the new lower side of the plasma membrane in columella cells, in which relocation of LAZY proteins from

the surface of amyloplasts to the adjacent plasma membrane is an important process. The repolarization of LAZY proteins induces asymmetrical auxin distribution and differential growth. When the roots resume vertical growth, the phosphorylation status and distribution of LAZY proteins return to their original state. The square frames indicate the root tips. The stars indicate the representative columella cells in root tips. Arrows labeled “G” indicate the direction of gravity.

KEY RESOURCES TABLE

REAGENT or RESOURCE	SOURCE	IDENTIFIER
Antibodies		
Mouse monoclonal anti-GST	CMC-TAG	Cat# AT0027
Mouse monoclonal anti-GST	Sigma-Aldrich	Cat# G1160
Mouse monoclonal anti-His	Sigma-Aldrich	Cat# H1029
Rabbit polyclonal anti-TxR	Cell Signaling Technology	Cat# 2351S
Rabbit polyclonal anti-LAZY4	This paper	N/A
Goat Anti-Rabbit Mouse IgG-HRP	Abmart	Cat# M21003
Bacterial and Virus Strains		
Trans5α Chemically Competent Cell	Transgen	Cat# CD201–01
Transetta (DE3) Chemically Competent Cell	Transgen	Cat# CD801–02
GV3101	Beyotime	Cat# D0392
Biological Samples		
Chemicals, Peptides, and Recombinant Proteins		
Murashige and Skoog Basal Medium	Sigma-Aldrich	Cat# M5519
Agar	Affymetrix USB	Cat# 10906
BASTA	Sigma-Aldrich	Cat# 45520
Hygromycin B	Thermo Fisher	Cat# 10687–010
MES hydrate	Sigma-Aldrich	Cat# M8250
$MgCl_2$•$6H_2O$	Sigma-Aldrich	Cat# M2670
$CaCl_2$	Sigma-Aldrich	Cat# C5670
D-Mannitol	Sigma-Aldrich	Cat# M4125
Poly (ethylene glycol)	Sigma-Aldrich	Cat# 81240
KCl	Sigma-Aldrich	Cat# P9541
LB broth	AmericanBio	Cat# AB01198–01000
Trizma Base	Sigma-Aldrich	Cat# T1503
NaCl	Sigma-Aldrich	Cat# S3014
Glucose	Sigma-Aldrich	Cat# C5767
Kanamycin sulfate	Amresco	Cat# 0408
Rifampicin	Sigma-Aldrich	Cat# R3501
Ampicillin	Amresco	Cat# 0339
Silwet L-77	GE Healthcare	Cat# SL77080596
SynaptoRed (FM4-64)	Millipore	Cat# C574799
Dimethyl sulfoxide	Sigma-Aldrich	Cat# D8418
DTT	Sigma-Aldrich	Cat# D0632
Protease inhibitors	Mei5bio	Cat# MF182
Phosphatase inhibitors	Mei5bio	Cat# MF183

REAGENT or RESOURCE	SOURCE	IDENTIFIER
RIPA buffer	Abcam	Cat# Ab156034
GFP-Trap beads	ChromoTek	Cat# gtma-20
Minimal SD Base	Takara	Cat# 630411
Minimal SD Base/Gal/Raf	Takara	Cat# 630420
DO Supplement-Ura	Takara	Cat# 630416
DO Supplement-His/-Trp/-Ura	Takara	Cat# 630424
RNeasy Plant Mini kit	Qiagen	Cat# 74904
DNeasy Plant Mini kit	Qiagen	Cat# 69104
X-gal	Takara	Cat# 9031
TRIS	VWR LifeScience	Cat# 0497
ExBlue Protein Stain	ZOMANBIO	Cat# ZD305A
Nonfat Dry Milk	Cell Signaling Technology	Cat# 9999
Clarity™ Western ECL Substrate	BIO-RAD	Cat# 170–5061
GST-tag Protein Purification Kit	Beyotime	Cat# P2262
His-tag Protein Purification Kit	Beyotime	Cat# P2226
IPTG	Sigma-Aldrich	Cat# I6758
SDS-PAGE Gel Preparation Kit	Coolaber	Cat# SK6010
Tween-20	Solarbio	Cat# T8220
PMSF	Mei5Bio	Cat# MF105
BSA	Sigma	Cat# B2064
ATP	NEB	Cat# P0756S
Glycine	VWR LifeScience	Cat# 0167
Deposited Data		
Raw peptide data	This paper, see www.proteomexchange.org	PXD045213
Experimental Models: Cell Lines		
Experimental Models: Organisms/Strains		
Arabidopsis lazy234–1	This paper	N/A
Arabidopsis lazy234–2	This paper	N/A
Arabidopsis lazy234–3	This paper	N/A
Arabidopsis ProLAZY2:LAZY2-GFP	This paper	N/A
Arabidopsis ProLAZY2:LAZY2-GFP/lazy234	This paper	N/A
Arabidopsis ProLAZY3:LAZY3-GFP/lazy234	This paper	N/A
Arabidopsis ProLAZY4:LAZY4-GFP/lazy234	This paper	N/A
Arabidopsis DR5rev::GFP	Ulmasov et al.[48]	N/A
Arabidopsis DR5rev::GFP/lazy234	This paper	N/A
Arabidopsis ProLAZY2:LAZY2ΔN-GFP/lazy234	This paper	N/A
Arabidopsis ProLAZY3:LAZY3ΔN-GFP/lazy234	This paper	N/A

REAGENT or RESOURCE	SOURCE	IDENTIFIER
Arabidopsis ProLAZY4:LAZY4ΔN-GFP/lazy234	This paper	N/A
Arabidopsis ProLAZY2:LAZY2-GFP/lazy234 pgm1	This paper	N/A
Arabidopsis ProLAZY3:LAZY3-GFP/lazy234 pgm1	This paper	N/A
Arabidopsis ProLAZY4:LAZY4-GFP/lazy234 pgm1	This paper	N/A
Arabidopsis pMPK3-MPK3-GFP	Huang et al.[45]	N/A
Arabidopsis mpk6$^{-/-}$ mpk3RNAi-est	Huang et al.[45]	N/A
Arabidopsis ProLAZY4:LAZY4-GFP/lazy23 mpk6$^{-/-}$ mpk3RNAi-est	This paper	N/A
Arabidopsis ProLAZY4:LAZY4-A 13-GFP /lazy234	This paper	N/A
Arabidopsis ProLAZY4:LAZY4-D9-GFP /lazy234	This paper	N/A
Arabidopsis ProTOC132:TOC132-RFP/ProLAZY4:LAZY4-D9-GFP/ lazy234	This paper	N/A
Arabidopsis ProLAZY4:LAZY4-D9-GFP/lazy234 toc120^{CR} toc132^{CR}	This paper	N/A
Arabidopsis ProLAZY4:LAZY4-GFP/lazy234 toc120^{CR} toc132^{CR}	This paper	N/A
Oligonucleotides		
Primers are listed in table S5	This paper	N/A
Recombinant DNA		
pHEE401E	Wang et al.[57]	N/A
p35S-Cas9-SK	Feng et al.[58]	N/A
pAtU6-26-M	Wang et al.[59]	N/A
pEC-Cas9	This paper	N/A
pCAMBIA 1300-LAZY2/3/4 sgRNA	This paper	N/A
pJIM19-LAZY2/3/4 sgRNA	This paper	N/A
pJIM19-ProLAZY2:LAZY2-GFP	This paper	N/A
pJIM19-ProLAZY3:LAZY3-GFP	This paper	N/A
pJIM19-ProLAZY4:LAZY4-GFP	This paper	N/A
pCAMBIA1300-ProLAZY2-LAZY2ΔN-GFP	This paper	N/A
pJIM19-ProLAZY3:LAZY3ΔN-GFP	This paper	N/A
pCAMBIA1300-ProLAZY4:LAZY4ΔN-GFP	This paper	N/A
pJIM19-ProLAZY4:LAZY4-A13-GFP	This paper	N/A
pJIM19-ProLAZY4:LAZY4-D9-GFP	This paper	N/A
pCAMBIA 1300-TOC132-mRFP	This paper	N/A
pUBQ10:Cas9-P2A-GFP (Gent)-TOC132-TOC120	This paper	N/A
pGEX4T-1-GST-LAZY2ΔCCL	This paper	N/A
pGEX4T-1-GST-LAZY3ΔCCL	This paper	N/A
pGEX4T-1-GST-LAZY4ΔCCL	This paper	N/A
pGEX4T-1-GST-LAZY4bh12ΔCCL	This paper	N/A
pGEX4T-1-GST-MKK5^{DD}	This paper	N/A
pGEX4T-1-GST-MPK3	This paper	N/A

REAGENT or RESOURCE	SOURCE	IDENTIFIER
pET28a-His-MKK5^{DD}	This paper	N/A
pET28a-His-MPK3	This paper	N/A
pB42-AD-LAZY4	This paper	N/A
pB42-AD-LAZY4-A5	This paper	N/A
pB42-AD-LAZY4-D5	This paper	N/A
pB42-AD-LAZY4-A9	This paper	N/A
pB42-AD-LAZY4-D9	This paper	N/A
pB42-AD-LAZY4-A13	This paper	N/A
pB42-AD-LAZY4-D13	This paper	N/A
plexA-BD-TOC33	This paper	N/A
plexA-BD-TOC34	This paper	N/A
plexA-BD-TOC64	This paper	N/A
plexA-BD-TOC75	This paper	N/A
plexA-BD-TOC90	This paper	N/A
plexA-BD-TOC120	This paper	N/A
plexA-BD-TOC132	This paper	N/A
plexA-BD-TOC132-GM	This paper	N/A
plexA-BD-TOC159-GM	This paper	N/A
Software and Algorithms		
Image J	NIH, USA	http://rsb.info.nih.gov/ij
R (version 4.2.2)	R Core Team (2022). Vienna, Austria.	https://www.R-project.org/
IBM SPSS statistics (version 24)	SPSS Inc., Chicago IL, USA	https://www.ibm.com/spss
Proteome Discoverer (versions 1.4, 2.2, 2.5)	Thermo Fisher	https://www.thermofisher.cn/cn/zh/home/industrial/mass-spectrometry/liquid-chromatography-mass-spectrometry-lc-ms/lc-ms-software/multi-omics-data-analysis/proteome-discoverer-software.html
MaxQuant (version 1.6.5.0)	Cox, J. and Mann, M (2008)	https://www.maxquant.org/
Other		
PVDF-Western Blotting Membranes	Roche Diagnostics	03010040001
PIP Strips	Echelon Biosciences	P-6001